الجمهورية الجزائرية الديمقراطية الشعبية

People's Democratic Republic of Algeria

وزارة التعليم العالي والبحث العلمي

Ministry of Higher Education and Scientific Research

المدرسة الوطنية العليا لعلوم البحر وتهيئة الساحل

Higher National School of Marine Science and Coastal Development

Thesis for the degree of Engineer and Master of Marine Science

Field: Natural and Life Sciences Marine and Continental Hydrobiology

Specialization: Aquaculture Management

Topic:

Energy Modeling and Sustainability Assessment of a Marine Aquaculture Farm Powered by Solar Energy

By:

ABDI Rayene Assala

BADJOUDJ Douaa

Defended on 10 /06/ 2026 before the following jury:

Ms. CHABET DIS	**Research Professor B**	**ENSSMAL**	**Chair**
Mr. DILMI	**Assistant Professor**	**ENSSMAL**	**Examiner**
Ms. MESLEM N.	**Senior Lecturer B**	**ENSSMAL**	**Advisor**

Academic Year: 2025/2026

Acknowledgments

First and foremost, we would like to express our deepest gratitude to our advisor, **Ms. MESLEM**. Much more than an advisor, she has been an exceptional teacher to us, whose scientific rigor, kindness, patience, and availability have left a lasting impression on our journey. Throughout working on this thesis, she guided us with professionalism, encouraged us to give our best, and imparted to us much more than knowledge: a genuine work methodology, a critical mindset and a commitment to scientific rigor. Her wise counsel, her constant support, and the trust she placed in us were instrumental in the completion of this work. We express our sincere gratitude and deep respect for all she has given us, both academically and personally.

We also extend our deepest thanks to **Ms. CHABET DIS** and **Mr. DILMI** for the honor they have bestowed upon us by agreeing to review and evaluate this work. We express our full gratitude for their availability as well as for the valuable lessons they have imparted to us throughout our academic journey.

We also extend our warmest thanks to **Mr. LOURGUIOUI** or his kind presence, his ongoing support and his dedication, despite his distance from our institution, which speaks to his scholarly generosity and his commitment to our success.

We would like to express our deepest gratitude to the CNRDPA team, particularly **Ms. ESSID** and **Ms. SEFFAH** , for their hospitality, their availability, and their invaluable collaboration throughout the various stages of this work.

We also extend our sincere thanks to the team at **ELECSUN** for their invaluable support during the completion of this work, particularly for providing the system's technical and economic data, as well as for their availability, patience, and constant collaboration.

Finally, we express our gratitude to all the professors who have guided us throughout our academic journey, each of whom has contributed, in their own way, to the development of our skills and the acquisition of a solid scientific methodology.

Finally, we would like to express our gratitude to the entire Higher National School of Marine Science and Coastal Development staff (ENSSMAL), for their guidance, their support and the favorable conditions provided to students throughout the program.

Dedications

Alhamdulillah, for giving me the strength, patience, and perseverance needed to get this far.

To my father, I love you deeply. You have been an essential anchor in my life, someone who taught me the strength, dignity, and courage to move forward without giving up. You have passed on values that shape me every day, and your trust has always been a source of motivation. Thank you for everything you do for me, even the things left unsaid. I love you.

To my mother, I owe you everything. You are the person who believed in me without ever hesitating, even when I doubted myself. You have been my strongest support, my anchor in difficult times, and the reason I have always picked myself up. A large part of what I have accomplished today is thanks to you. You taught me kindness, gentleness, and patience through the way you are. Thank you for your love, your sacrifices, and your constant presence. I love you.

To my brothers, Mohamed, Hachem, and Lotfi, you are an essential part of my life and my sense of balance. Mouh, you are so much more than a brother my first and eternal best friend, the one I grew up with and shared so much with, a presence I've always been able to count on. Hachem and Lotfi, you are my pillars, my anchors, and my strength in everyday life. You have always been there for me, and your presence gives me the energy and courage to move forward. I love you.

To my sister Hidaya, I love you deeply. You are a strong person, and that strength inspires me deeply. I want you to know that I will always be there for you. I wish you the very best for your future. I love you deeply.

To my best friends Lina (Douaa), Fadhela, Douaa, and Houda, thank you for always being by my side, for your support, and for your kindness. You have been a true source of strength and inspiration to me, and I hold you very dear in my heart. I love you so much.

To Sofia, Hana, Khaoula, Nada, Nawel, and Faten, thank you for being in my life and for the beautiful moments we've shared. Despite our differences, you've created sincere bonds based on respect, solidarity, and understanding. You've shown me the value of good company—the kind that uplifts and leaves a beautiful mark on the heart. I pray for each of you, from the bottom of my heart, that Allah grants you success and the fulfillment of your dreams.

ABDI Assala Rayene

To my dear mother, one of the greatest women I know: strong, resilient, and yet infinitely gentle. Her love and trust have been my guiding light in moments of doubt and the source of my courage.

To my father, my sisters, my brother, my uncle, my aunts, and my grandparents, I offer my deepest gratitude for your unconditional love and constant support throughout this journey.

To my best friends, whom I love more than anything: Assala, my partner in this work and a precious friend it was an honor to share this project with you. Douaa, my lifelong friend, whose loyalty and companionship have made life lighter and memories more beautiful. Rosa and Hiba, your smiles, your kindness, and your infectious joy have brightened my everyday life. Thank you for listening, for your support, and for the moments of happiness we shared.

Finally, to my classmates who have become wonderful friends: Hanna, Khaoula, Sofia, and Nada. Thank you for making these university years a richer, happier, and unforgettable experience.

Douaa Badjoudj

Abstract

This study addresses the energy modeling and sustainability assessment of a solar-powered marine aquaculture farm, using the experimental Recirculating Aquaculture System (RAS) facility of the National Center for Research and Development of Fisheries and Aquaculture (CNRDPA) as a case study.A hybrid photovoltaic system was sized and optimized using HOMER Pro (Hybrid Optimization of Multiple Energy Resources) software and real site data. Simulation results show that the optimized configuration (211 kW PV, 1,612 batteries) achieves an 84.6% renewable fraction, a Levelized Cost of Energy (LCOE) of 4.40 DA/kWh (22.3% below grid tariff), a 9.1-year payback period, and an 84.7% emissions reduction. An Arduino-based monitoring system was also developed. Solar integration in intensive aquaculture proves a viable lever for reducing costs, fossil fuel dependence, and environmental impact in Algeria.

Résumé

ملخص Cette étude porte sur la modélisation énergétique et l'évaluation de la durabilité d'une exploitation aquacole marine alimentée à l'énergie solaire, en prenant comme étude de cas l'installation expérimentale de système aquacole en recirculation (RAS) du Centre national de recherche et de développement pour la pêche et l'aquaculture (CNRDPA). Un système photovoltaïque hybride a été dimensionné et optimisé à l'aide du logiciel HOMER Pro (Hybrid Optimization of Multiple Energy Resources) et de données réelles du site. Les résultats de la simulation montrent que la configuration optimisée (211 kW PV, 1 612 batteries) permet d'atteindre une part d'énergies renouvelables de 84,6 %, un coût actualisé de l'énergie (LCOE) de 4,40 DA/kWh (22,3 % en dessous du tarif du réseau), un délai de récupération de 9,1 ans et une réduction des émissions de 84,7 %. Un système de surveillance basé sur Arduino a également été développé. L'intégration de l'énergie solaire dans l'aquaculture intensive s'avère être un levier viable pour réduire les coûts, la dépendance aux combustibles fossiles et l'impact environnemental en Algérie.

ملخص

تتناول هذه الدراسة نمذجة الطاقة وتقييم الاستدامة لمزرعة تربية الأحياء المائية البحرية التي تعمل بالطاقة الشمسية، وذلك باستخدام منشأة نظام تربية الأحياء المائية المعاد تدويرها (RAS) التجريبية التابعة للمركز الوطني للبحث والتطوير في مجال مصايد الأسماك وتربية الأحياء المائية كحالة دراسية. وقد تم تحديد حجم نظام كهروضوئي هجين وتحسينه باستخدام برنامج تحسين الأنظمة الطاقوية الهجينة وبيانات الموقع الفعلية. تُظهر نتائج المحاكاة أن التكوين المُحسّن (211 كيلوواط من الطاقة الكهروضوئية و1612 بطارية) يحقق نسبة طاقة متجددة تبلغ 84.6٪، وتكلفة طاقة مُعادلة تبلغ 4.40 دينار جزائري لكل كيلوواط ساعة (أقل بنسبة 22.3٪ من تعريفة الشبكة)، وفترة استرداد تبلغ 9.1 سنة، وخفضًا في الانبعاثات بنسبة 84.7٪. كما تم تطوير نظام مراقبة قائم على المتحكم المصغر. وقد أثبت دمج الطاقة الشمسية في تربية الأحياء المائية المكثفة أنه وسيلة فعالة لتقليل التكاليف والاعتماد على الوقود الأحفوري والتأثير البيئي في الجزائر.

Table of Contents

List of Tables

List of Figures

List of Abbreviations

Abbreviations	**Meaning**
IEA	International Energy Agency (IEA)
AC	Alternating Current (AC)
DC	Direct Current (DC)
UNFCCC	United Nations Framework Convention on Climate Change (UNFCCC)
NDC	Nationally Determined Contribution (NDC)
CNDPA	National Center for Fisheries and Aquaculture Development (predecessor of CNRDPA)
CO_2	Carbon dioxide
COE	Cost of Energy
COP21	Conference of the Parties – 21st session
DC	Direct Current
DOE	Department of Energy
EIA	Energy Information Administration
EJ	Exajoule (unit of energy = 10^{18} joules)
EPST	Public Scientific and Technological Institution
FAO	Food and Agriculture Organization of the United Nations
GHG	Greenhouse Gas (GHG)
IPCC	Intergovernmental Panel on Climate Change (IPCC)
GW	Gigawatt (unit of power = 10^9 watts)
HOMER	Hybrid Optimization of Multiple Energy Resources
IDE	Integrated Development Environment
IEA	International Energy Agency
JORA	Official Journal of the Algerian Republic

KBM	Kinetic Battery Model
kW	Kilowatt (unit of power = 10^3 watts)
kWh	Kilowatt-hour (unit of energy)
LCD	Liquid Crystal Display
LCOE	Levelized Cost of Energy
MW	Megawatt
NDC	Nationally Determined Contribution
NO_2	Nitrogen Dioxide
NO_x	Nitrogen Oxides
NPC	Net Present Cost
NREL	National Renewable Energy Laboratory (United States)
NSRDB	National Solar Radiation Database (NREL)
OECD	Organization for Economic Cooperation and Development (OECD)
SDGs	Sustainable Development Goals (SDGs)
WHO	World Health Organization (WHO)
UN	United Nations (UN)
$PM_{2.5}$	Fine particulate matter with a diameter of less than 2.5 micrometers
PSH	Peak Sun Hours
PV	Photovoltaic
PVWatts	Online photovoltaic simulation tool developed by NREL
RAS	Recirculating Aquaculture System
SO_2	Sulfur Dioxide
TWh	Terawatt-hour (unit of energy = 10^{12} Wh)
UNECE	United Nations Economic Commission for Europe

UV	Ultraviolet radiation
WAPI	World Aquaculture Policy Initiative

Introduction

1. The Global Energy Imperative and Its Impact on the Sector

Energy is a fundamental driver of economic and industrial development. The transition of energy systems from traditional sources to fossil fuels has led to significant productivity gains but has now resulted in a dual crisis linked to resource depletion and environmental impacts, particularly greenhouse gas emissions (IPCC, 2023).

In this context, the transition to renewable energy is emerging as a strategic and environmental necessity (UN, 2022), particularly in energy-intensive sectors where energy directly determines system performance.

In Algeria, this shift is reflected in a strategy aiming for 15 GW of renewable capacity by 2035 (Hakima Kaddour, 2024), driven by the country's solar potential.

2. Intensive aquaculture and the constraints of RAS systems

Aquaculture now plays a central role in global food security, with production exceeding that of capture fisheries (FAO, 2024; OECD-FAO, 2023). Among production systems, RAS offers high control over rearing conditions and improved water efficiency.

However, their operation relies on a major constraint: the continuous maintenance of stable physicochemical conditions to ensure the well-being of the fish. This requires a constant energy supply for recirculation, aeration, filtration, and thermal regulation (Badiola et *al*., 2012).

Thus, energy represents both a cost factor and a critical condition for the biological stability of the system.

3. Aquaculture in Algeria: Ambitions and Energy Constraints

The relationship between national aquaculture ambitions and the imperative of energy transition lies at the heart of the issue addressed in this thesis. Algerian intensive aquaculture farms are currently powered by the national electricity grid, nearly all of whose production comes from natural gas (IEA, 2021). This dependence on fossil fuels results in significant operational costs, vulnerability to price fluctuations and grid incidents, as well as greenhouse gas emissions that are difficult to reconcile with the sector's stated sustainability goals.

Replacing a significant portion of this consumption with photovoltaic energy, while maintaining the absolute power supply reliability required by RAS systems, represents a complex technical and economic challenge. This challenge cannot be met by a simple solar installation without storage: the intermittency of PV is structurally incompatible with the continuous nature of the aquaculture load.

It requires the rigorous design of a hybrid system integrating solar generation, battery storage, and grid backup, optimized simultaneously from technical, economic, and environmental perspectives.

4. Research Objective and Thesis Structure

This thesis, entitled "Energy Modeling and Sustainability Assessment of a Marine Aquaculture Farm Powered by Solar Energy," presents an energy modeling and sustainability assessment study using the experimental farm of the National Center for Research and Development in Fisheries and Aquaculture (CNRDPA) in Bou Ismail (Tipaza) as a case study. In the absence of any renewable energy production system within this facility, this study proposes the design and optimization of a hybrid system, tailored to the specific energy constraints of the aquaculture operation, using HOMER Pro software and based on actual data on electricity consumption and solar irradiance.

Beyond the technical, economic, and environmental analysis, this work proposes a smart energy management approach based on the availability of solar resources. In this context, a low-cost solar irradiance monitoring and decision-support system was designed using Cirkit Designer. Based on Arduino-style control logic, this device aims to support energy load management by suggesting certain energy-intensive activities during periods of high photovoltaic production, to improve self-consumption and the overall efficiency of the system.

Chapter I : Generalties

1.1 Background and Challenges of Aquaculture

1.2 The Role of Aquaculture Worldwide

Aquaculture has become a pillar of global aquatic food production, not only by meeting the growing demand for seafood but also by helping to alleviate pressure on wild fisheries.

In 2022, global aquaculture production reached a record high of 130.9 million tons, including 94.4 million tons of aquatic animals and 36.5 million tons of algae. It is worth noting that this is the first time that aquaculture production of aquatic animals for human consumption has exceeded that of capture fisheries (FAO, 2024).

Fish is the main source of protein for approximately 950 million people worldwide and constitutes a significant part of the diet for many others. Historical trends indicate that between 1970 and 2010, global per capita fish consumption nearly doubled. Currently, fish accounts for about 16% of the animal protein consumed worldwide and provides essential minerals and fatty acids (Pradeepkiran, 2019).

1.3 Aquaculture in Algeria

1.3.1 Historical Overview and Production Profile

In Algeria, aquaculture has a rich and evolving history spanning over a century, reflecting gradual development and increasing sophistication (Bouguerra, 2023).

Algeria's contribution to global aquaculture production is relatively small, accounting for 0.0044% of total production, even though it represents 1.78% of the world's land area and 0.56% of the world's population (World Aquaculture Policy Initiative [WAPI], 2023).

Between 2000 and 2020, Algeria's aquaculture production rose from 351 tons to 5,436 tons, representing an annual growth rate of 14.68%, exceeding subregional, regional, and global averages, as well as those of neighboring countries (WAPI, 2023). This growth was primarily driven by marine aquaculture, whose share increased from 13.4% to 64.2% (WAPI, 2023).

Algerian marine aquaculture has a potential annual production capacity of 120,000 tons, although current production remains between 6,000 and 7,000 tons. The Ministry of Fisheries has approved nearly 200 projects, 70 of which are currently under development, which has increased marine aquaculture production from 3,000 tons in 2022 to 6,000 tons today , the government aims to double production to reach 100,000 tons per year by 2030 (Hana Saada, 2024).

Despite these achievements, the FAO emphasizes the need to implement ongoing adaptation strategies to improve the efficiency, inclusivity, resilience, and sustainability of aquatic food systems, which are essential for combating food insecurity, reducing poverty, and ensuring effective governance of aquatic resources (Hana Saada, 2024).

1.4 Aquaculture systems and their energy consumption

1.4.1 Types of Aquaculture Systems

Aquaculture systems range from very extensive systems to semi-intensive and highly intensive systems, including hyper-intensive systems. When using this terminology, it is important to define the specific characteristics of each system, as there are no clear distinctions and levels of intensification represent a continuum (Funge-Smith & Phillips, 2001).

Farming systems are also diverse, for example:

- Aquatic systems (cages and pens, coastal/offshore). (Funge-Smith & Phillips, 2001).
- Land-based systems (rainwater ponds, irrigated or recirculating systems, tanks, and canals). (Funge-Smith & Phillips, 2001).
- Recirculating systems (highly controlled closed systems, more open recirculation based on ponds). (Funge-Smith & Phillips, 2001).
- Integrated farming systems (e.g., livestock and fish farming, dual-purpose aquaculture for agriculture and fish farming, and irrigation ponds) (Funge-Smith & Phillips, 2001).

1.5 Recirculating Aquaculture Systems (RAS)

1.5.1 Components and Operation

Recirculating aquaculture is essentially a technology that allows fish or other aquatic organisms to be raised by reusing water in production. This technology relies on the use of mechanical and biological filters, and the method can in principle be used for all species farmed in aquaculture, such as fish, shrimp, clams, etc. (FAO, 2022).

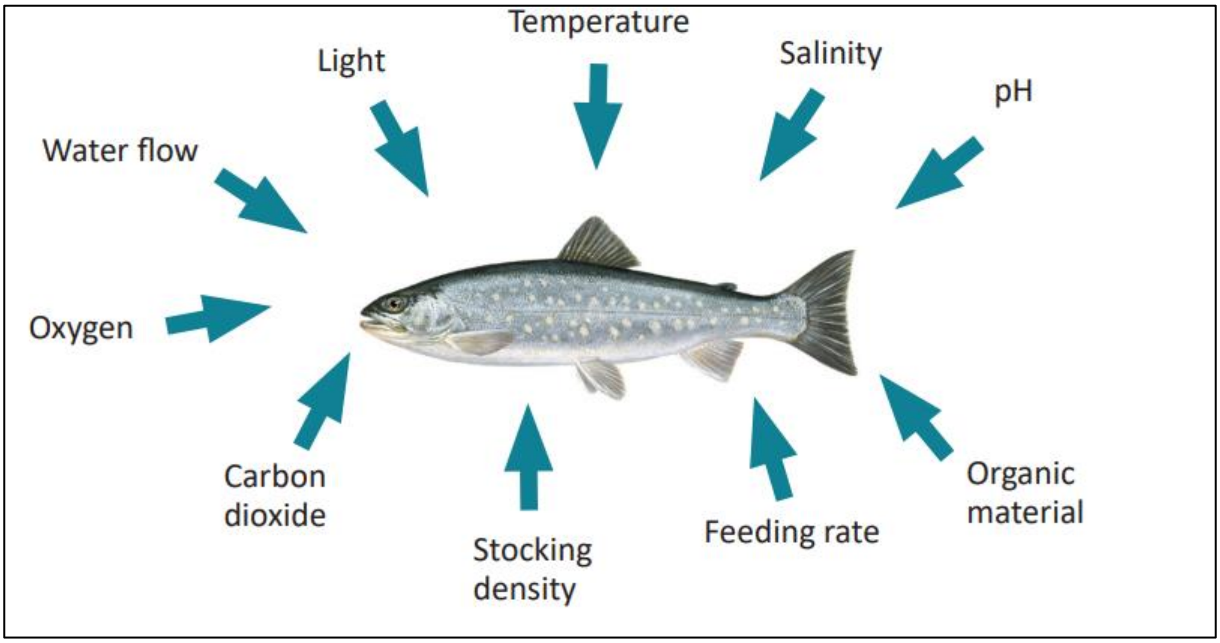

Figure1 . Parameters influencing the growth and welfare of farmed fish (FAO, 2022)

Recirculation allows fish farmers to fully control all production parameters (Fig. 1), and their skills in operating the recirculation system become just as important as their ability to care for the fish (FAO, 2022).

Maintaining water temperature, oxygen, and light at optimal levels reduces stress in the fish and promotes steady growth, allowing for accurate prediction of their size and time of sale. This improves farm management and competitiveness (FAO, 2022).

The impact of pathogens is significantly reduced in a recirculating system, as invasive diseases from the external environment are minimized by the limited use of water (FAO, 2022).

A recirculating aquaculture system (RAS) consists of several interconnected components, each performing a specific function to maintain water quality and optimal conditions for fish production (FAO, 2022).

Figure 2 illustrates the components of a recirculating aquaculture system (FAO, 2022).

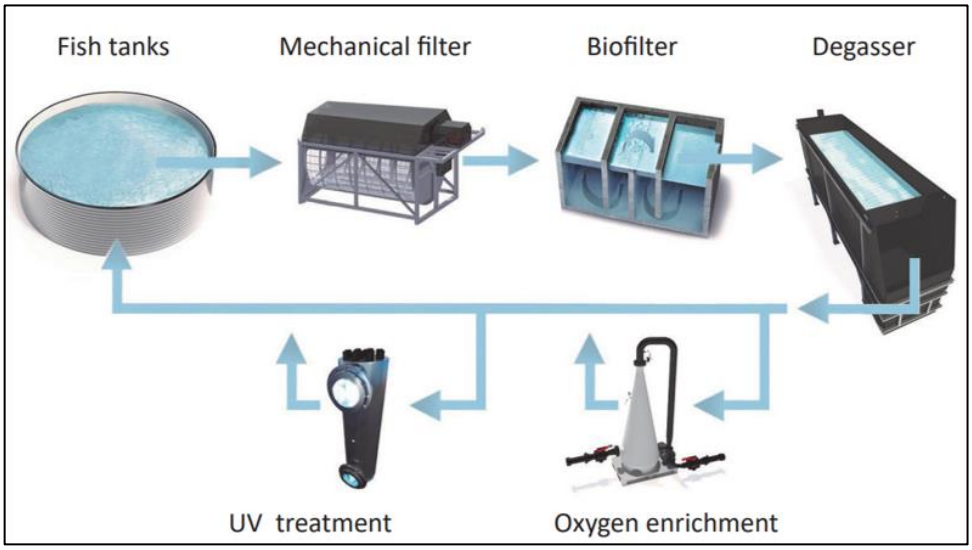

Figure2 . Schematic diagram of a recirculation system (FAO , 2022)

The basic water treatment system includes mechanical filtration, biological treatment, and degassing. Other facilities, such as oxygenation or UV treatment, can be added as needed (FAO, 2022).

1.5.2 Environmental benefits

Reduced environmental impact: control of eutrophication, reduced emissions, and optimized waste management through reduced discharge volumes (Badiola et *al*., 2018).

Optimization of water use: a drastic reduction in water consumption, a significant advantage in a context where water resources are becoming scarce (FAO, 2022).

Nutrient recovery: collection of nutrients derived from livestock farming that can serve as agricultural fertilizers or be used to generate biogas, thereby contributing to a circular economy approach (FAO, 2022).

1.6 Energy Challenges in Aquaculture

The efficiency of recirculating aquaculture systems (RAS) is closely linked to their energy consumption, which is one of the most critical operational factors. To maintain optimal water quality, high recirculation rates are necessary; however, increased water exchange and treatment intensity inevitably lead to higher energy demand, particularly for the pump and water circulation. It is therefore crucial to conduct a thorough analysis of the system’s energy consumption to determine the most effective operational strategies and reduce overall energy consumption without compromising production efficiency (David et *al*., 2009).

1.7 Energy and Sustainability

1.7.1 Global Energy Context and Environmental Challenges

1.7.2 Definition and Sources of Energy

Energy, the capacity to perform work, is crucial for individual and social development. A country's energy level often serves as an indicator of its development (Mekuye et *al*., 2024). It powers homes, transportation, and industries, and is essential for economic growth, technological progress, and quality of life, while also needing to meet environmental and sustainability goals (Mekuye et *al*., 2024).

The energy system encompasses production, distribution, and use, with major importance for:

- Economic growth: industrial support and development (Mekuye et *al*., 2024).
- Sustainability: transition to renewable and more efficient energy sources (Mekuye et *al*., 2024).
- National security: energy independence (Mekuye et *al*., 2024).
- Public health: reduction of pollution-related risks (Mekuye et *al*., 2024).
- Resilience: continuity of essential services (Mekuye et *al*., 2024).

Non-renewable Energy Sources

Non-renewable energy sources are resources consumed faster than they can be replenished, primarily fossil fuels and nuclear energy (Mekuye et *al*., 2024).

Renewable Energy Sources

Renewable energy comes from naturally recurring and sustainable energy flows present in the environment (Fig. 3). Renewable energy is often referred to as green or sustainable energy (Osman et *al*., 2022).

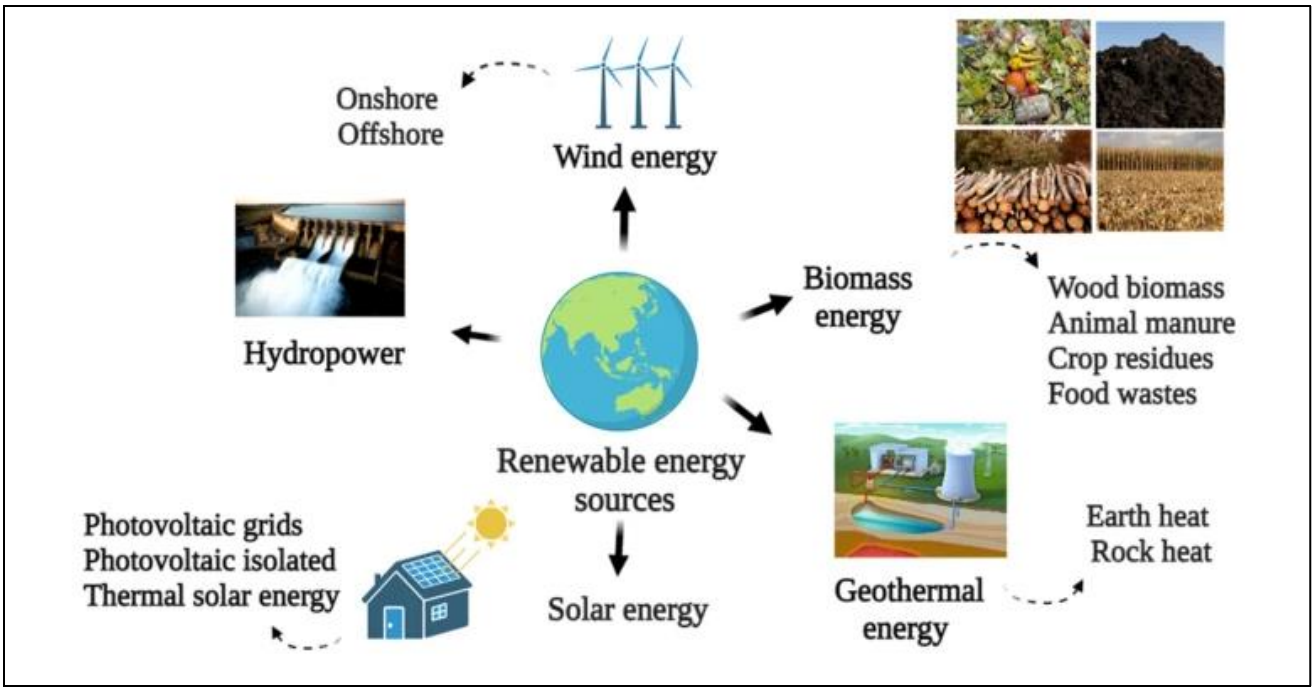

Figure3 . Renewable energy sources (Osman et *al*, 2022)

1.7.3 Global Energy Demand and Current Trends

Global energy demand is rising due to population growth and industrialization. In 2024, it increased by 2.2%, driven primarily by electricity consumption, and could double by 2050. Renewables account for 38% of this increase, but fossil fuels remain the dominant source in the global energy mix (IEA, 2025).

In 2024, global electricity demand grew by 4.3%, exceeding growth rates of previous years and reflecting the rise of electrification across all sectors. China remains the main driver, but all regions recorded growth above their recent annual average. In total, global electricity consumption increased by 1,080 TWh, nearly double the average of the previous decade (IEA, 2025).

1.8 Environmental Impacts of Electricity Generation

In 2024, the energy sector, dominated by natural gas and coal, produced 37.8 Gt of CO_2, pushing atmospheric concentrations to 422.5 ppm , a 50% increase from pre-industrial levels (Guidi et *al.*, 2023; IEA, 2025).

In Algeria, electricity generation accounted for 31% of energy-related CO_2 emissions in 2023, primarily from the combustion of natural gas and, to a lesser extent, coal (IEA, 2024).

Electricity generation by natural gas combined-cycle power plants, without carbon capture, emits between 403 and 513 g CO_2eq per kWh, with over 80% of this emitted during combustion. Each kilowatt-hour of electricity consumed therefore generates approximately 400 to 500 grams of CO_2 into the atmosphere (UNECE, 2022).

Natural gas combined-cycle power plants consume large amounts of water for cooling, which can pose a problem in regions where water is scarce, particularly when competing with agriculture and municipalities (Macknick et *al*., 2012).

1.9 The Importance of the Energy Transition to Renewable Energy

Heavy reliance on fossil fuels leads to serious environmental impacts such as global warming, deforestation, and pollution (Climate and Clean Air Coalition & Health, Climate & Air Pollution, 2025)

Renewable energy sources, particularly solar and wind power with battery storage, are now more competitive than fossil fuels in most countries (World Economic Forum, 2025) and provide universal access to electricity, promoting regional energy self-sufficiency and improving living conditions, health and education, particularly in rural areas (Royal Society of Chemistry, 2025; Tokyo Institute of Technology, 2025).

1.9.1 International Framework: Paris Agreement and Sustainable Development Goals

The Paris Agreement represents a major milestone in the fight against climate change. Adopted on December 12, 2015, by 196 parties at COP21 and entered into force on November 4, 2016, it aims to limit the global temperature increase to below 2°C, or even 1.5°C, compared to pre-industrial levels. It requires each country to submit national climate targets. As of September 2023, 94 countries and the European Union have made a legally binding commitment to climate neutrality, while others have developed non-binding strategies (Guidi et *al*., 2023).

This focus on sustainable energy is particularly relevant to food production, where the link between energy and production has become increasingly critical. Aquaculture, the fastest-growing sector of animal food production, is highly energy-intensive and requires significant inputs for water circulation, aeration, heating and cooling, feeding systems, and post-harvest processing (Ayer & Tyedmers, 2009).

1.10 Renewable Energy in Aquaculture

1.10.1 Fossil Fuel Dependence and Energy Demand in Aquaculture

Conventional aquaculture systems rely heavily on fossil fuels, particularly petroleum, diesel, and other non-renewable energy sources. The sector's energy costs and associated carbon emissions have drawn increasing attention in recent years (Vo et *al*., 2021).

1.10.2 The Role of Renewable Energy in Sustainable Aquaculture

The transition from fossil fuels to renewable energy sources is considered one of the most promising strategies for increasing the sustainability of food systems and mitigating climate change (Scroggins et *al*., 2022).

Renewable energy comes from natural processes that are constantly replenished, such as sunlight, geothermal heat, wind, tides, water flow, and biomass. These sources are inexhaustible and constantly regenerate. Often referred to as "clean" or "green" energy, they produce minimal environmental pollution. Integrating renewable energy into aquaculture operations can reduce production costs and improve the overall sustainability of farms (Bharathi et *al*., 2019).

1.10.3 Overview of Renewable Energy Options for Aquaculture

Within this diverse landscape of renewable energy sources, solar energy stands out as one of the most accessible and adaptable options for aquaculture applications (Isaac, 2025).

1.10.3.1 Solar Energy

Solar radiation can be converted into thermal or electrical energy using mechanical or photovoltaic devices. The adoption of solar energy in aquaculture can improve operational efficiency, reduce energy costs, and increase farm resilience while supporting environmentally sustainable practices (Isaac, 2025).

1.10.4 Relevance of Solar Energy for the Aquaculture Sector

According to the World Energy Council (2013), the total solar energy incident on Earth exceeds the total global annual primary energy consumption (which is 450 EJ) by more than 7,500 times.

- **Reduced operating costs**

By harnessing freely available solar radiation, farms can reduce their electricity and fuel expenses, resulting in substantial long-term financial savings (Isaac, 2025).

- **Increased energy independence and reliability**

Frequent power outages can lead to deteriorating water quality and potential fish losses. Solar photovoltaic systems, particularly when combined with battery storage, provide a stable and independent power supply. This energy self-sufficiency ensures optimal environmental conditions (Isaac, 2025).

- **Environmental benefits**

The use of solar energy directly reduces the environmental footprint of aquaculture activities. By replacing electricity generated from fossil fuels, solar photovoltaic systems reduce greenhouse gas emissions, thereby contributing to climate change mitigation (Isaac, 2025).

- **Scalability and Versatility**

Solar photovoltaic technology is highly adaptable, ranging from small panels that power individual pumps or lights to large-scale installations that supply energy to the entire farm's operations (Isaac, 2025).

1.10.5 Application of solar energy in aquaculture

1.10.6 Hybrid Solar Systems

Hybrid photovoltaic systems combine two or more complementary energy technologies to improve the reliability of the energy supply. Since renewable sources such as the sun do not provide a constant supply of energy, hybrid systems help ensure a more stable electricity supply over time (Hasnaoui & Benrouissi, 2018).

1.11 Solar Energy Potential in Algeria:

Algeria has significant solar potential due to its favorable geographic location, which makes it one of the sunniest regions in the world. Annual sunshine hours generally exceed 2,000 hours across most of the country, reaching up to 3,900 hours in the highlands and the Sahara. This abundance of solar radiation corresponds to an estimated daily energy yield on a horizontal surface area of 1 m² of approximately 5 kWh, with annual totals of about 1,700 kWh/m² in the northern regions and 2,263 kWh/m² in the south (Haddad & Boulahchiche, 2025).

1.11.1 Challenges and Strategic Prospects for the Solar Energy Sector in Algeria

Algeria has struggled to fully implement its 2015–2030 energy program, leading to its revision with a new target of 15,000 MW by 2035. This is largely due to structural and socio-technical constraints linked to the country's historical dependence on hydrocarbons; despite the challenges, Algeria's solar photovoltaic program offers significant opportunities, not only for energy production but also for industrial development (Haddad & Boulahchiche, 2025).

Chapter II: Materials and Methods

2 Materials and Methods

2.1 Presentation of the CNRDPA Experimental Farm and The RAS System

The National Center for Research and Development in Fisheries and Aquaculture (CNRDPA) is a Public Scientific and Technological Institution (EPST) located in Bou Ismaïl (Tipaza Province, Algeria) (Fig. 4), operating under the supervision of the Ministry of Fisheries and Aquaculture. Resulting from the restructuring of the CNDPA, it was officially established in 2008 by Executive Decree No. 08-128 of April 30, 2008, establishing the standard status of the EPST.

As part of its statutory missions, the CNRDPA works to develop scientific knowledge and decision-support tools through a rigorous research approach grounded in the operational realities and environmental constraints specific to the sector. It thus contributes to the sustainable growth of fisheries and aquaculture, while ensuring the preservation of production environments (CNRDPA, 2026).

The Bou Ismaïl Marine Fish Farming Experimental Station was established as part of the expansion of the CNRDPA's research activities. It specializes in the reproduction and rearing of marine fish such as sea bream (*Sparus aurata*), sea bass (*Dicentrarchus labrax*), striped seabass (*Argyrosomus regius*), and turbot (*Scophthalmus maximus*), as well as in research on grouper (*Epinephelus marginatus*), mullet (*Mugil cephalus*), and sole (*Solea senegalensis*).

Figure4 . Location of the marine fish farming experimental station (CNRDPA, Bou Ismaïl) (Google Earth)

2.2 Architectural Layout of the Facility

The aquaculture facility consists of several units operating in a recirculating aquaculture system (RAS), dedicated to the different phases of the rearing cycle, notably the larval, juvenile, nursery, and reproduction stages (Fig. 5). Each unit comprises tanks of varying volumes, connected to recirculation systems incorporating various water treatment equipment, such as mechanical filters (sand and drum filters), biological filters, skimmers, circulation pumps, and UV sterilizers. In some cases, thermal regulation devices, such as heat pumps, are also used.

The water supply is provided by a pumping station with a capacity of approximately 100 m³/h, supported by several pumps, and supplemented by a 200 m³ storage tank as well as a settling system.

In addition, specific facilities are dedicated to the production of live feed. Microalgae are cultured in small-volume containers using thermal sterilization systems with 2000 W heating elements. Rotifers are produced in tanks equipped with 500 W heating elements, which maintain a stable temperature of around 25 °C. Similarly, the production of Artemia relies on several tanks equipped with comparable heating devices.

Finally, although the cold room is currently out of service, the tanks are aerated by blowers, ensuring adequate oxygenation conditions .

Figure5 . Architectural plan of the experimental farm of CNRDPA (Baz & Laouas, 2025)

The general layout of the production spaces and technical areas is illustrated in Figure 5, providing a visual representation of the facility's overall structure.

2.3 Status of The Station's Technical Infrastructure

The CNRDPA aquaculture station is a semi-functional experimental farm, organized into closed-loop (RAS) and semi-open production units. These units cover the various stages of the sea bream and sea bass rearing cycle, from weaning to the nursery, and consist of tanks of varying sizes combined with appropriate recirculation systems. The infrastructure notably includes pump rooms, a storage tank, shaded areas for the cultivation of microalgae, rotifers, and artemia, as well as a cold storage room. The partially operational status of this equipment determines the station's overall performance and directly influences its energy profile .

2.3.1 Non-functional Facilities

Part of the infrastructure remains out of service, limiting the site's production capacity and energy efficiency. Non-operational facilities include several concrete tanks, the microalgae cultivation greenhouse, the open-loop system's machine room, and two laboratories. The table below summarizes these facilities:

Table1 . Non-functional facilities at the hatchery (Baz & Laouas, 2025)

Type of facility	Number
3.5 m³ concrete broodstock tanks	12
Concrete broodstock tanks 9.5 m³	4
16 m³ concrete broodstock tanks	2
Concrete weaning tanks 2.8 m³	24
Concrete quarantine tanks 5.6 m³	2
Concrete pre-fattening tanks 16 m³ (under a greenhouse)	12
Microalgae cultivation greenhouse	1
Open-loop machine room	1

2.3.2 Operational Facilities

The units still in operation allow for the continuation of essential activities such as larval and post larval rearing, nursery operations, and reproduction. They are equipped with tanks connected to filtration systems (sand filters, biological filters, skimmers), UV sterilizers, and circulation pumps. The water supply is provided by a temporary pumping station with a capacity of 100 m³/h, supplemented by a 200 m³ reservoir and settling tanks .

2.4 Organization and Functions of the Rearing Rooms

2.4.1 Incubation and Larval Rearing Room

The central hub of the aquaculture cycle, this room is divided into two zones: egg incubation and larval rearing. The incubation zone is equipped with four 350-liter cylindrical-conical polypropylene incubators, and the larval rearing zone features four 1,700-liter cylindrical polypropylene tanks, along with a recirculation module comprising pumps, filters, a skimmer, a UV sterilizer, and a heat pump. The continuous operation of this equipment, which is essential for maintaining sanitary and biological conditions, makes it one of the center's most energy-intensive sectors (Fig. 6) .

Figure6 . Incubation and larval rearing room (CNRDPA)

2.4.2 Weaning Room

Designed for post-larval rearing, it comprises eight 1,700-liter cylindrical polypropylene tanks. Water circulation in a closed loop is provided by three pumps, ensuring stable quality parameters. This continuous operation results in significant electricity consumption, directly linked to the development of the juveniles (Fig. 7).

Figure7 . Weaning room at the National Center for Research and Development in Aquaculture (CNRDPA)

2.4.3 Nursery and Pre-grow-out Room

These two areas house eight cylindrical polypropylene tanks, each with a capacity of 3,700 L. The recirculation system includes pumps, mechanical and biological filters, a skimmer, a UV sterilizer (Fig. 8), and a heat pump. The system ensures a stable environment for growth but represents significant energy consumption due to the volume of water treated and the constant temperature regulation (Fig. 9) .

Figure8 . UV sterilizer in the pre-fattening room (CNRDPA)

Figure9 . Nursery and pre-enlargement room (CNRDPA)

2.4.4 Microalgae Culture Room

Cultivation is carried out in containers ranging from 0.5 to 20 L, with aeration via air pumps and thermal sterilization (heating to 75 °C or autoclaving). These processes, essential for sanitary quality, involve continuous electricity consumption, particularly due to heating elements (Fig. 10) .

Figure10 . Microalgae culture room (CNRDPA)

2.4.5 Rotifer Room

Equipped with five 1,400-liter cylindrical polypropylene tanks and six 700-liter tanks, this room produces the zooplankton used as live feed. Oxygenation is provided by air pumps, circulation by water pumps, and the temperature is maintained at 25 °C using heating thermostats. Maintaining these biological conditions at a constant level result in significant energy consumption (Fig. 11) .

Figure11 . Rotifer breeding room at the Centre National de Recherche et de Développement en Aquaculture (CNRDPA)

2.4.6 Artemia Room

Comprising six 350-liter cylindrical-conical polypropylene tanks, this room uses air pumps for oxygenation and heating thermostats to maintain the water at 28 °C, an essential condition for cyst hatching. (Fig. 12).

Figure12 . Artemia room at the National Center for Research and Development in Aquaculture (CNRDPA)

2.5 Operation of The Closed-loop Recirculation System

The closed-loop recirculation system is the heart of the aquaculture facility, ensuring water quality and the stability of biological parameters essential for farming. This operation relies on a series of treatment steps, each utilizing specific equipment (Fig. 13) and generating continuous energy consumption.

Water from the grow-out tanks is first conveyed by gravity to a rotating drum filter, which mechanically filters out suspended solids. It is then collected in a buffer tank before being pumped to a sand filter and subsequently disinfected by a UV sterilizer. The water then passes through a biological filter, where the nitrification process converts ammonia into nitrites and then into nitrates, which are less toxic to fish. Finally, a reversible heat pump regulates the temperature, providing heating or cooling as needed.

A protein skimmer, equipped with an independent pump, completes the system by removing organic matter through skimming. All of this equipment operates continuously, which guarantees the water’s sanitary quality but results in an unavoidable energy load (Fig. 14) .

This continuous operation of the system makes it a critical component in energy analysis and justifies the exploration of hybrid solutions incorporating photovoltaic power generation to reduce dependence on the grid.

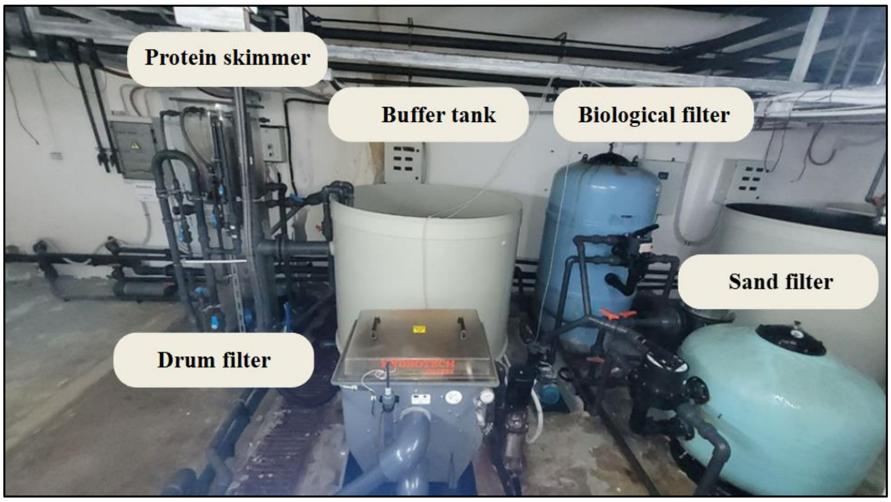

Figure13 . Water filtration and treatment system – Weaning room (CNRDPA)

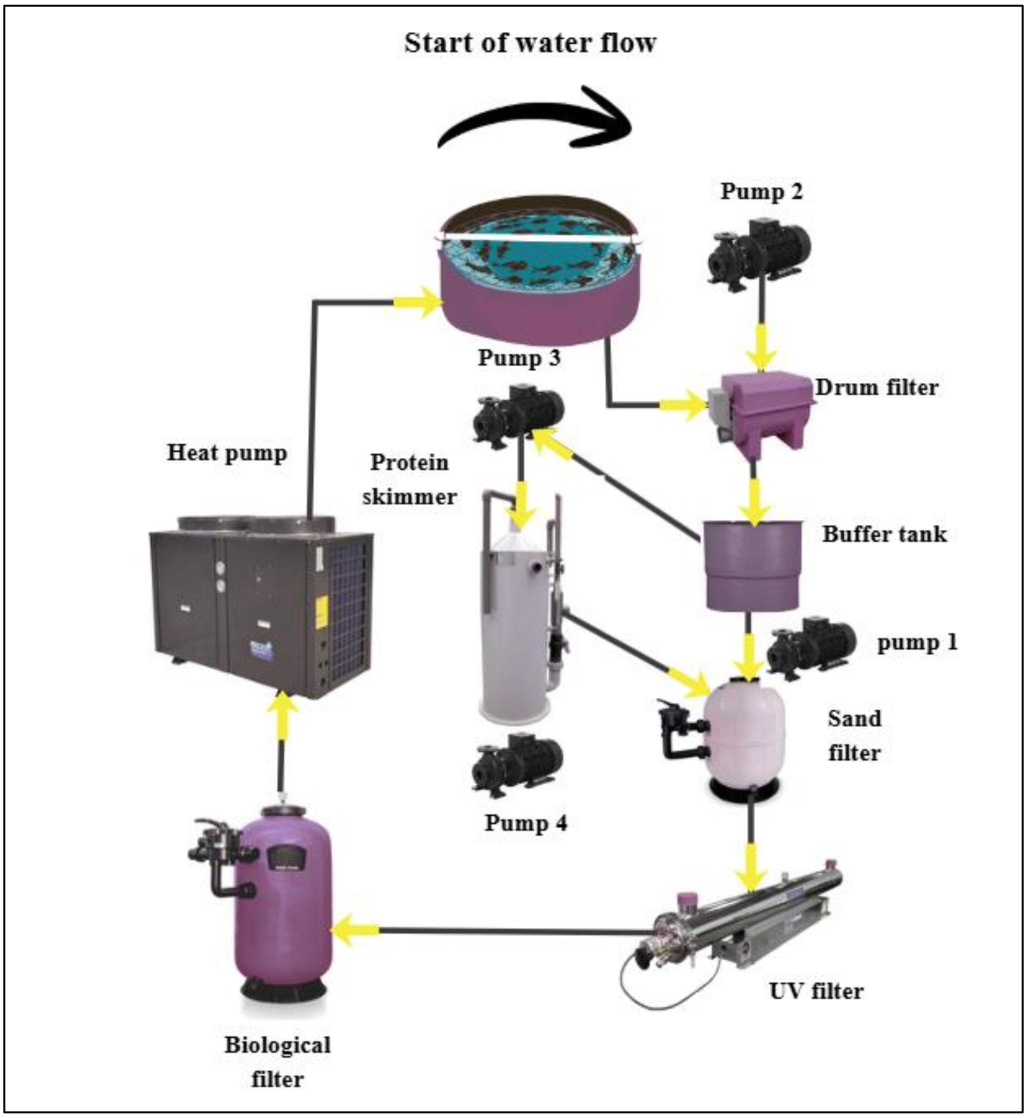

Figure14 . Schematic diagram of the closed-loop aquaculture system at the CNRDPA

2.6 The HOMER Pro Simulation Tool

HOMER Pro (version 3.14.2) is a widely recognized simulation and optimization software for the design of hybrid energy systems based on renewable energy. Initially developed by the USA's National Renewable Energy Laboratory (NREL), it has become a go-to tool for researchers, engineers, and decision-makers involved in the planning of decentralized energy systems. Its main advantage lies in its ability to assess both the technical feasibility and economic performance of complex microgrid configurations, thereby facilitating the identification of optimal energy mixes for isolated areas or those with limited access to the power grid (Fig. 15) (Biswas et *al*., 2026).

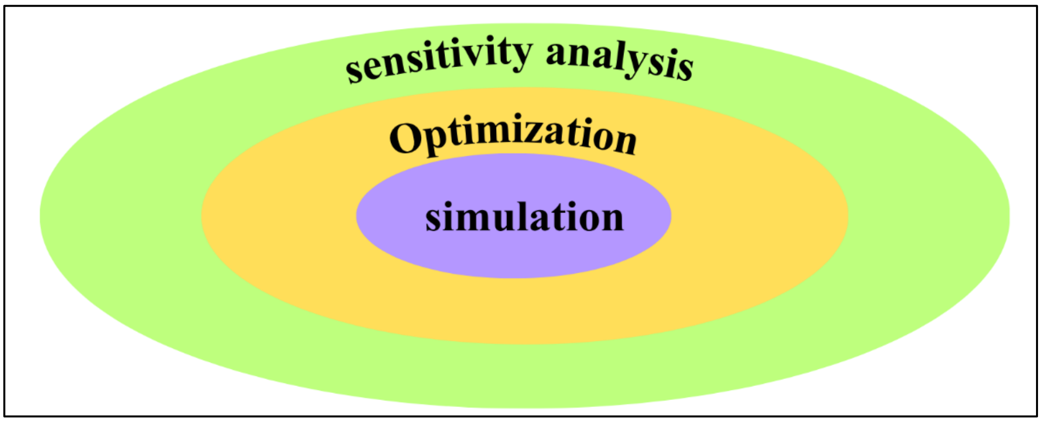

Figure15 . Conceptual model of the HOMER software (Lalwani et *al*., 2010)

HOMER Pro can be expanded with customizable modules, including: biomass, hydropower, combined heat and power (CHP), advanced loads, advanced grid, hydrogen, advanced storage, multi-year analysis, and integration with MATLAB (Homer Energy, 2020).

The software is capable of modeling a wide range of energy technologies, including photovoltaic systems, wind turbines, battery storage systems, biomass generators, as well as emerging technologies such as hydrogen-based systems. HOMER Pro evaluates multiple system configurations based on key input parameters such as the availability of local renewable resources, electricity load profiles, component characteristics, and operational constraints. It then performs an optimization process to identify the most appropriate configurations (Fig. 16), using key economic indicators such as net present cost (NPC) and cost of energy (COE), with the aim of determining the most economically viable and reliable solution (Biswas et *al*., 2026).

HOMER Pro also incorporates life-cycle cost analysis, battery degradation effects, and an assessment of the system's environmental impact. This ensures that the optimized configurations are not only cost-effective but also sustainable in the long term (Biswas et *al*., 2026).

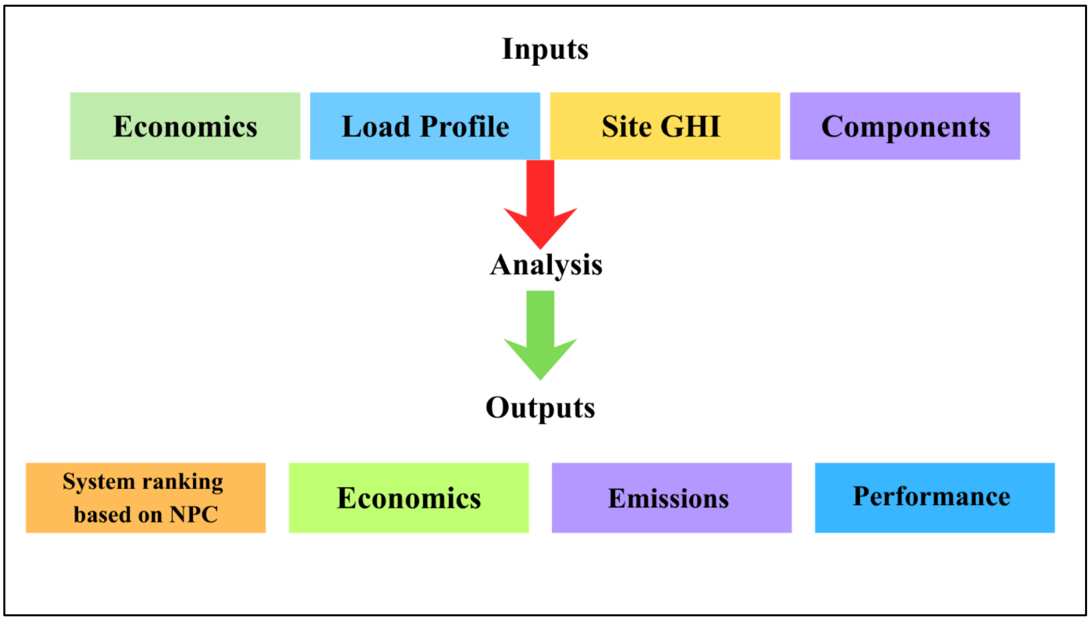

Figure16 . Flow diagram of Homer Pro software simulation (This study)

2.7 Energy modeling and sizing of the hybrid photovoltaic system

2.7.1 Reference energy data

To establish an energy model of the system, actual electricity consumption data from the National Aquaculture Research Center of Bou Ismaïl (CNRDPA) were used. These data were obtained from electricity bills and cover three representative years (2016, 2018, and 2019). For the analysis, only the year 2019 was selected as the reference period, due to consistent and representative aquaculture activity during that time.

2.7.2 Breakdown by Equipment Category

The figure (Fig. 17) below illustrates the distribution of installed electrical power by equipment category within the CNRDPA. This representation highlights the dominant energy-intensive items (pumps, incubators, heating/cooling systems), confirming their critical role in the load profile and guiding the energy management strategy.

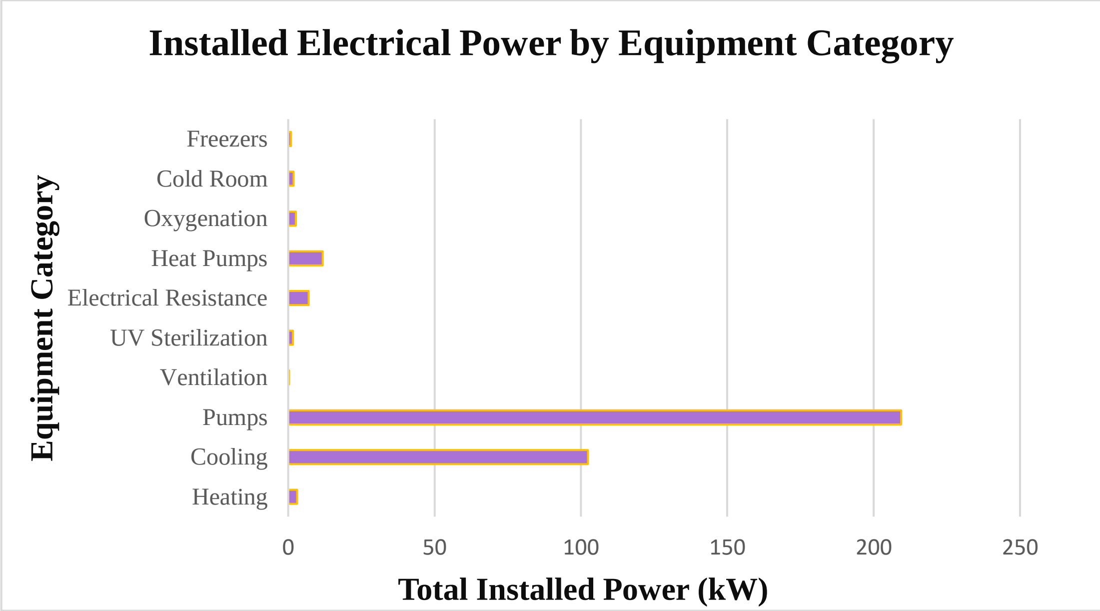

Figure17 . Breakdown of installed electrical power by equipment category at the CNRDPA

2.7.3 Data Processing

To enable integration into the simulation tool, monthly consumption (kWh/month) was converted into hourly load profiles (kW/h) by distributing it evenly across the 2hours of each month.

2.7.4 Characterization of the solar resource

The site's solar resource was characterized using data from PVWatts.

2.7.5 PVWatts

PVWatts (version 8.4.1) an open source tool that was developed by the USA's National Renewable Energy Laboratory (NREL) as a simplified simulation tool for estimating the energy production of grid-connected photovoltaic systems (Fig. 18). It uses meteorological data from NREL and the National Solar Radiation Database (NSRDB) to generate site-specific performance estimates. Energy production is calculated based on key system parameters such as installed capacity, tilt angle, and azimuth orientation (Raji et al., 2025).

By integrating solar resource data with standardized performance assumptions, PVWatts provides consistent and reliable estimates of photovoltaic energy production while requiring only a limited number of input variables. This makes it particularly well-suited for feasibility studies and the preliminary evaluation of PV projects (Raji et al., 2025).

Figure18 . PVWatts® calculator homepage

PVWatts provides the following outputs:

- Monthly solar radiation on the collector plane (kWh/m²/day) (Raji et *al*., 2025)
- Monthly and annual alternating current (AC) power generation (kWh) (Raji et *al*., 2025)
- System configuration parameters (installed capacity, tilt, and azimuth) (Raji et *al*., 2025)
- Performance indicators such as the DC capacity factor (Raji et *al*., 2025)
- System loss assumptions (including inverter, temperature, and cabling losses) (Raji et *al*., 2025)
- Power generation profiles at different time resolutions, depending on the selected output format (Raji et *al*., 2025)

Overall, PVWatts is an effective and practical tool for the preliminary evaluation of photovoltaic systems, supporting early-stage decision-making in the development of solar energy projects (Raji et *al*., 2025).

2.7.6 Data Extraction Methodology

The following parameters were entered into PVWatts to simulate system generation:

2.7.7 Solar resource data

- Site: Tipaza, Algeria
- Latitude/Longitude: 36.65° N; 2.7° E

2.7.8 System info

- Module type: Standard
- Installation type: Fixed (open rack)
- System DC power: 253.5 kW, determined using the System Size Estimator tool (Fig. 19)
- System losses: 14.08% (calculated using the Loss Calculator)
- Tilt: 37° (corresponding to the site's latitude)
- Azimuth: 180° (south-facing)

Figure19 . Estimation of installable DC power based on roof area using the System Size Estimator (PVWatts)

2.7.9 Expected results

Based on these parameters, PVWatts provides:

- Average monthly and annual solar radiation (kWh/m²/day)
- Monthly and annual AC energy produced by the system (kWh)
- Total annual AC energy production, which serves as the basis for comparison with the CNRDPA's energy demand

2.7.10 Reference parameters for photovoltaic modules

2.7.11 Choice of photovoltaic module

The modules used are based on bifacial N-type monocrystalline technology, enabling additional energy production via the rear side, with an estimated gain of between 5% and 25% depending on installation conditions. The module efficiency reaches approximately 23%, with a bifaciality factor of around 80%.

2.7.12 Electrical Characteristics (STC)

Under standard test conditions (STC: 1000 W/m², 25°C, AM 1.5), the main electrical parameters are as follows:

- Rated power: 600 W
- Maximum power voltage (Vmpp): ≈ 44.5 V
- Maximum power current (Impp): ≈ 13.4 A
- Open-circuit voltage (Voc): ≈ 52 V
- Short-circuit current (Isc): ≈ 14.2 A
- Efficiency: ≈ 23%

2.7.13 Physical characteristics

The modules measure 2278 × 1134 × 30 mm, corresponding to an area of approximately 2.58 m², and weigh 27 kg.

2.7.14 Thermal characteristics

Thermal performance is characterized by a power temperature coefficient of -0.29%/°C, indicating a decrease in power as temperature increases. The nominal operating cell temperature (NOCT) is approximately 45 °C.

2.7.15 Durability and Performance

The modules exhibit annual degradation limited to approximately 0.4%, with a performance guarantee of 87.4% after 30 years, ensuring good long-term durability.

2.7.16 PV System Sizing Methodology

The sizing of a photovoltaic system depends primarily on the energy demand to be offset, the local solar resource (expressed in Peak Sun Hours), and the system's overall efficiency (degradation factor). These parameters allow for estimating the optimal capacity of a photovoltaic array based on the site's specific needs. The methodology applied in this study is based on recommendations from the University of Maryland Extension, which provides a simplified and reproducible procedure for estimating the size and output of a PV system (University of Maryland Extension, 2023).

2.7.17 Energy Modeling and Sizing Steps

1. Determine the annual energy demand Based on electricity consumption data, expressed in kWh/year.
2. The solar offset represents the fraction of annual energy demand that you wish to offset with photovoltaics; the target solar energy is obtained by multiplying annual consumption by this coefficient.
3. Calculate the ideal system power: Divide the desired solar energy by the site's annual *Peak Sun Hours*.
4. Accounting for the derating factor: The ideal system power must be adjusted by a derating factor to account for the system's actual inefficiencies.
   A default value of 86% (0.86 in decimal form) is commonly used.
5. The capacity of the photovoltaic system is calculated based on annual consumption, *Peak Sun Hours* (PSH), the *solar offset*, and the *derate factor*.
6. Estimating the number of PV panels:
   Once the system capacity has been determined, it is possible to estimate the number of modules required. This estimate is made by dividing the total system power by the nominal power of a single panel. A conversion factor is required (1 kW = 1,000 W).

2.7.18 Energy Coverage Scenarios

Two solar coverage scenarios were selected for sizing the photovoltaic system:

- **Scenario 1:** 50% energy coverage This scenario corresponds to partial offsetting of annual electricity demand through photovoltaics.

- **Scenario 2:** 65% energy coverage This scenario aims for greater offsetting, allowing for a further reduction in grid dependence.

2.7.19 Verification of available space for the photovoltaic installation

The available surface area was verified by comparing the estimated total roof area (≈1,334 m^2) with the area required to accommodate the photovoltaic modules in the two scenarios studied.

2.8 Modeling and optimization of the hybrid system using HOMER Pro

The simulations were performed using HOMER Pro under a free trial license. The model was developed based on the aquaculture site's annual electricity demand, solar resource data obtained from PVWatts, and the technical specifications of the photovoltaic modules, inverters, and battery storage system. These inputs formed the basis of the energy modeling process and enabled the evaluation of the selected energy coverage scenarios.

2.8.1 Simulation Inputs in HOMER Pro

The modeling presented in this section corresponds to the 65% energy coverage scenario.

The diagram shown below (Fig. 20) was configured after sizing all the components of the hybrid system, taking into account the electrical load of the aquaculture site (CNRDPA), the power grid, the photovoltaic modules, the inverter, and the battery.

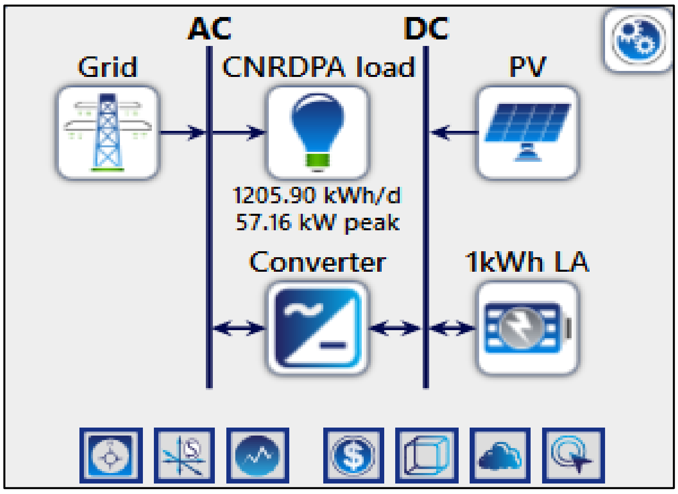

Figure 20. Diagram of the PV-grid hybrid system (HOMER Pro)

The HOMER Pro microgrid model for the CNRDPA was configured with the site coordinates 36°39.0'N, 2°41.6'E (Bou Ismail, Algeria). The project lifetime was set to 30 years, with a discount rate of 8.00% and an inflation rate of 2.00% (both default values computed by HOMER Pro). The primary AC load had a scaled annual average of 1,205.90 kWh/day and a peak of 57.16 kW. Grid electricity was priced at 5.660 DA/kWh with no sellback. The system included a converter costing 2280 000 DA with 96.00% efficiency, and a battery bank of 112 lead-acid units (1 kWh each) at a total capital cost of 168 000 DA.

2.9 Performance Indicators

Most of the time, the performance of photovoltaic (PV) systems is measured using a set of indicators that compare the system's output to its theoretical maximum under normal operating conditions. These indicators provide a way to numerically measure the system's performance and efficiency (Odeh, 2018).

The traditional method for evaluating the operation of an energy generation system involves comparing the energy actually produced over a certain period (e.g., a day, a month, or a year) to the maximum amount of energy it could produce over that same period. This method works for traditional energy production systems, such as power plants using fossil fuels and those using renewable energy, but photovoltaic systems must be considered differently. Variations in sunlight and the impact of weather conditions significantly influence the operational efficiency and energy production of photovoltaic systems over time (Odeh, 2018). Consequently, the literature proposes several specific performance indicators to account for these characteristics.

The indicators adopted in this study, based on previous research, are summarized below:

2.9.1 System Efficiency (η_system)

System efficiency is defined as the ratio of the electrical energy generated by the photovoltaic system to the total solar radiation incident on the surface of the PV field (Odeh, 2018).

2.9.2 Solar Fraction (SF)

The solar fraction is defined as the ratio of the energy produced by the photovoltaic system to the total energy demand of the site in question (Odeh, 2018).

2.9.3 Capacity Factor (CF)

The capacity factor is defined as the ratio of the photovoltaic system's actual annual energy production to the energy that would be produced if the system operated continuously at its rated power throughout the year (Odeh, 2018).

2.9.4 Final System Efficiency (Yf)

The final system efficiency is defined as the ratio of the PV system's net electrical energy production to the DC rated power of the installed PV array (Marion et *al*., 2005).

The final system efficiency is used to normalize the energy production of a PV system relative to its installed capacity, allowing for a comparison between systems of different sizes (Marion et *al*., 2005).

2.9.5 Reference Efficiency (Yr)

The reference efficiency is defined as the ratio of total solar radiation on the collector plane to the reference solar radiation (Marion et *al*., 2005).

2.9.6 Performance Ratio (PR)

The performance ratio is defined as the ratio of the system's final yield to the reference yield (Marion et *al*., 2005).

2.10 Economic evaluation (via HOMER Pro)

Economic modeling in HOMER is a fundamental component for assessing the bankability and profitability of various energy system configurations. By systematically evaluating the costs and benefits associated with various combinations of generation technologies, the model enables stakeholders to make informed investment decisions regarding the adoption of clean and sustainable energy solutions (Biswas et *al*., 2026).

The system payback period is used to assess the time required to recoup the initial investment. It is defined as the ratio of the initial investment (or the asset's original cost) to annual cash inflows(Biswas et *al*., 2026).

A shorter payback period indicates a more economically efficient system, reflecting a faster recovery of the invested capital (Biswas et *al*., 2026).

2.10.1 Net Present Cost (NPC)

The Net Present Cost represents the system's overall economic performance over its lifetime. It is defined as the difference between the total present value of all costs incurred over the project's duration and the total revenue generated. A negative NPC value indicates that the system is economically profitable. The economic performance of each configuration is primarily evaluated using the Net Present Cost (NPC) (Biswas et *al*., 2026).

2.10.2 Net Present Value (NPV)

It is used as a comparative indicator between system configurations. This metric allows for the evaluation of the economic benefits obtained by the proposed system compared to a reference configuration (Biswas et *al*., 2026).

2.10.3 Levelized Cost of Energy (LCOE)

The Levelized Cost of Energy (LCOE) represents the average cost of energy production over the system's lifetime (Biswas et *al*., 2026).

2.10.4 Internal Rate of Return (IRR)

The Internal Rate of Return (IRR) is a metric used to assess the system's profitability over its lifetime (Biswas et *al*., 2026).

2.10.5 Renewable Fraction (RF)

The renewable fraction (RF) represents the share of energy supplied by renewable sources relative to the system's total production (Biswas et *al*., 2026).

2.11 Environmental Assessment

Environmental assessment plays a crucial role in evaluating the sustainability of energy systems. Emissions of greenhouse gases such as carbon dioxide (CO_2), nitrogen oxides (NO_x), and sulfur dioxide (SO_2), primarily resulting from the use of non-renewable energy sources, contribute significantly to climate change and air pollution.

2.12 Load Management Strategy

To complement the photovoltaic sizing study and support operational decision-making at the aquaculture farm level, a low-cost solar radiation monitoring and alert system is proposed as part of the energy management strategy. The system architecture was designed and wired using the Cirkit Designer integrated development environment.

Chapter III:

Results and Discussion

3 Results and Discussion

3.1 CNRDPA Electricity Consumption Profile

The graph below (Fig. 21) shows monthly energy consumption (kWh) for the year 2019. Total annual consumption reached 440,189 kWh, with a monthly average of 36682 kWh.

The months of July (40569 kWh) and August (42529 kWh) show the highest consumption levels, reflecting an increase in aquaculture activities during the summer months (pumping, aeration, temperature control).

April (30059 kWh) and December (32636 kWh) show the lowest values, corresponding to reduced energy needs during periods of lower activity.

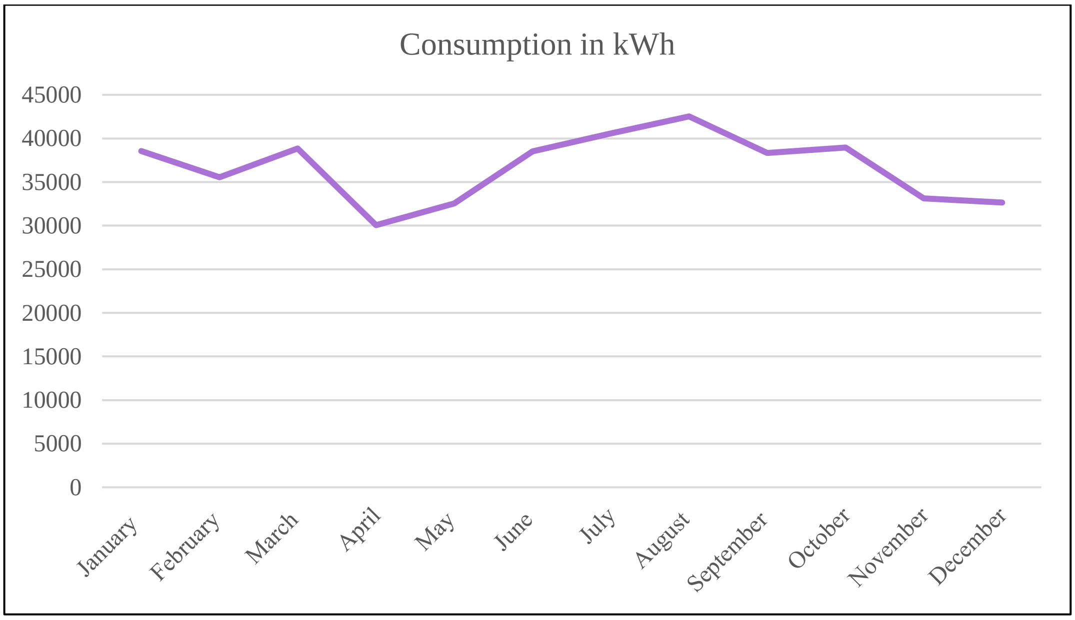

Figure 21. Monthly electricity consumption at the CNRDPA for the year 2019 (kWh) (Baz & Laouas, 2025)

The graph (Fig. 22) illustrates the trend in monthly electricity costs at the CNRDPA for the year 2019.

- The total annual cost amounts to 2533010 DZD, with a monthly average of 211084 DZD.
- The months of July (228564 DZD) and August (239024 DZD) show the highest values, corresponding to the period of high energy consumption observed in the previous graph.
- April (180838 DZD) shows the lowest cost, consistent with the decrease in consumption (30059 kWh).

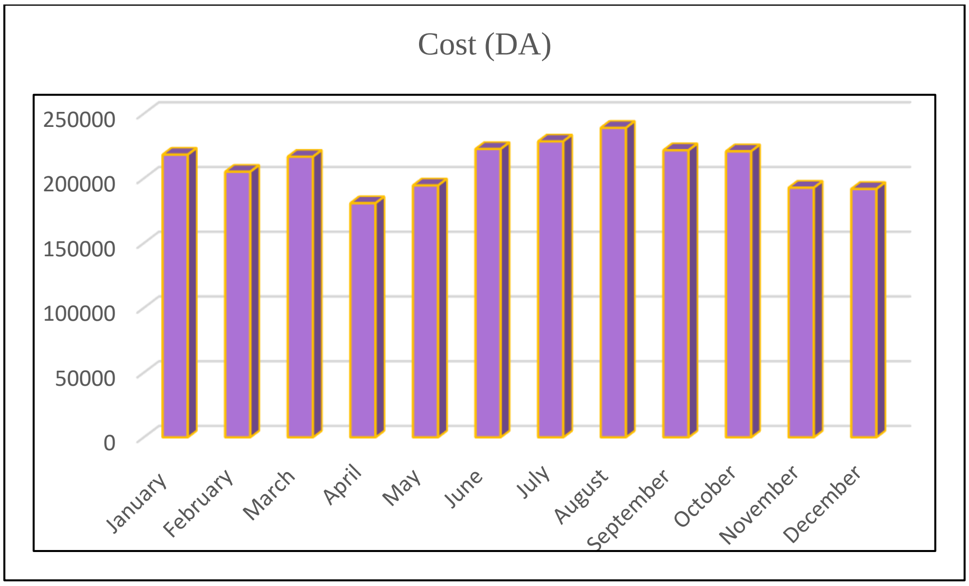

Figure 22. Monthly electricity cost at the CNRDPA for the year 2019 in Algerian dinars (DA) (Baz & Laouas, 2025)

3.2 Hourly Electricity Consumption Profile

Monthly consumption data (kWh/month) were successfully converted into hourly load profiles (kW/h) for integration into HOMER Pro. The weighted annual average is 1205.90 kWh/day, with a peak of 57.16 kW.

The continuous, uninterruptible nature of the aquaculture load constitutes the most fundamental design constraint in this study. RAS systems require a 24-hour power supply with zero tolerance for outages, as any interruption would result in fish mortality due to anoxia (Emezirinwune et *al*., 2024).

This constraint, which is absent in residential or commercial applications, justifies the use of storage and grid backup as non-optional components of the system design.

3.3 Economic Input Data for HOMER Pro Simulation

To ensure that the economic analysis reflects actual market conditions, the cost data used in this study were obtained directly from ELECSUN, an Algerian company specializing in the supply and installation of photovoltaic systems. ELECSUN provided accurate and up-to-date pricing for all system components, including photovoltaic panels, mounting structures, cabling, installation services, and inverters. These data were integrated into HOMER Pro to evaluate the proposed 600 W PV system under two scenarios: Scenario 1, corresponding to a 50% renewable share, and Scenario 2, corresponding to a 65% renewable share.

3.4 PVWatts Simulation Results – Irradiance and AC Output

The solar potential of the Tipaza site is favorable, with an average annual irradiance of 5.39 kWh/m²/day. Annual photovoltaic production amounts to 376,958 kWh.

The value of 5.39 kWh/m²/day falls within the reported range, with 5.01 kWh/m²/day in Sidi-bel-Abbès and 5.30 kWh/m²/day in Laghouat (Fezzani et *al*., 2023).

A seasonal breakdown shows that solar availability is lowest in fall, increases in spring, reaches its maximum in summer, and decreases again in winter. These variations correspond closely with the farm's energy demand profile, with summer offering the most balanced match between solar supply and consumption, while fall and winter require greater reliance on the grid.

3.5 PV System Sizing

Based on annual consumption data (440189 kWh/year) and local solar conditions (PSH = 5.39 h/day, or 1967.35 h/year), the optimal capacity of the photovoltaic array was estimated taking into account a derating factor of 0.86. Two energy coverage scenarios were selected:

- **Scenario 1 (50% coverage)**: an installed capacity of 130.2 kW, corresponding to approximately 217 600-W modules. The total area required is 560.5 m².
- **Scenario 2 (65% coverage)**: an installed capacity of 169.2 kW, corresponding to approximately 283 600-W modules. The total area required is 730.9 m².

3.6 Verification of The Available Area for The Photovoltaic Installation

Verification of the available area for the photovoltaic installation shows that the roof area required is approximately 560.5 m² for Scenario 1 (50% coverage) and approximately 730.9 m² for Scenario 2 (65% coverage). Given that the total roof area is estimated at approximately 1 334 m², both scenarios are physically feasible.

3.7 Performance Indicators

To evaluate the technical performance of the two configurations studied, several indicators were calculated based on the PVWatts simulation results for 600 W panels. The values obtained for scenarios S1 (50%) and S2 (65%) are presented in Table 2.

Table2 . Performance metrics calculated for 600 W panel configurations

Performance indicator	600 W – S1 (50%)	600 W – S2 (65%)
System efficiency (η_system)	19.98	19.93
Solar fraction (SF)	50.0%	65.0

Capacity factor (CF)	19.32	19.32
Final efficiency (Yf)	1692.3 h	1692.4 h
Reference yield (Yr)	1967 h	1967 h
Performance Ratio (PR)	0.86	0.86

The performance indicators obtained for the 600 W panel configurations demonstrate solid technical performance in both scenarios. The system efficiency values, 19.98% and 19.93% for Scenarios 1 and 2, respectively, fall within the accepted range for industrially produced monocrystalline silicon modules, which achieve actual efficiencies of 20–22% (U.S. Department of Energy, 2024). The solar fraction (SF) values of 50.0% and 65.0% are consistent with comparable literature, where average annual SF values of approximately 68.5% have been reported for grid-connected systems of similar design (Odeh, 2018). The capacity factor of 19.32%, identical in both scenarios, reflects the favorable solar resources at the Bousmail site and is comparable to the 20.79% recorded for a grid-connected photovoltaic power plant under Algerian climatic conditions (Bendaas et *al*., 2025).

The reference yield obtained at Bou Ismaïl in both scenarios (Yr = 1967 h/year) is consistent with the values reported by (Fezzani et *al*., 2023), who measured 1,829 h/year in Sidi-bel-Abbès and 1935 h/year in Laghouat.

The final yield obtained at Bou Ismaïl in both scenarios (Yf ≈ 1692 h/year) is comparable to the values reported by (Fezzani et *al*., 2023), who measured 1515 h/year at Sidi-bel-Abbès and 1710 h/year at Laghouat.

The performance ratio obtained (PR ≈ 0.86) is identical for both scenarios. This value falls within the range of 0.6 to 0.9 generally reported in the literature for grid-connected photovoltaic systems (Odeh, 2018). This result confirms that the system simulated for the Tipaza site exhibits high efficiency and limited losses.

3.8 HOMER PRO Optimization Results

The 65% scenario was selected as the reference for optimization, as it allows a larger portion of energy needs to be met by photovoltaic electricity. This choice aims to maximize the contribution of renewable energy while remaining compatible with the available surface area and the site's technical constraints.

HOMER ranks all system configurations in its optimization results based on the total NPC (Fig. 23), which represents the present value of all costs incurred over the project's lifetime minus all revenues generated, and serves as the primary basis for system selection (Dodo et *al*., 2024).

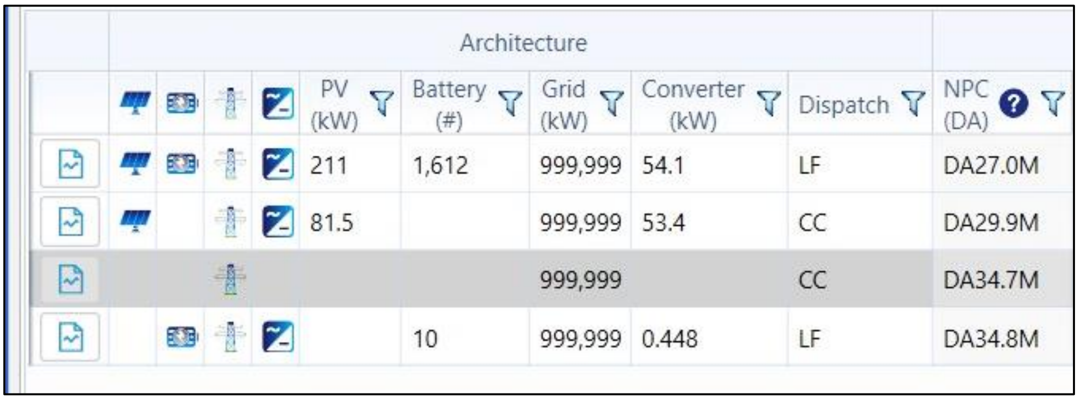

Architecture									
				PV (kW)	Battery (#)	Grid (kW)	Converter (kW)	Dispatch	NPC (DA)
				211	1,612	999,999	54.1	LF	DA27.0M
				81.5		999,999	53.4	CC	DA29.9M
						999,999		CC	DA34.7M
					10	999,999	0.448	LF	DA34.8M

Figure 23.HOMER optimization results for selected system configurations

The results presented in the optimization table clearly indicate that the configuration combining 211 kW of photovoltaic panels, 1612 batteries, and a 54.1 kW converter under the load-following (LF) strategy constitutes the optimal system architecture.

To assess the economic viability of the proposed system, HOMER Pro was used to estimate the total project costs over its 30-year lifespan. Table 3 summarizes the key economic indicators obtained for the two analyzed scenarios: the baseline scenario based solely on the utility grid, and the optimized hybrid system selected as the lowest-cost solution.

Table3 . Comparative analysis of economic indicators over the project's lifetime

Economic indicator	Baseline scenario (network only) (DA)	Optimized hybrid system (Lowest-cost system) (DA)
NPC (total cost over 30 years)	34 700 000	27 042 820
LCOE	5.66/kWh	4.40/kWh
Initial capital (CAPEX)	0	16 700 000
Annual operating and maintenance costs	2490000/year	743 513/year

3.9 Net Present Cost (NPC)

The net present cost (NPC), as shown in Table 4, reveals a clear economic advantage for the proposed hybrid system compared to the scenario where system is grid connected. The optimized configuration has a total life-cycle cost of 27.0 million DA over 30 years, compared to 34.7 million DA for the grid-only scenario, representing a reduction of aproximately 7.7 million DA in present value. Thus, the NPC of the hybrid system is 22.2% lower than that of the grid-only scenario, confirming the economic superiority of this configuration in the long term. For various Algerian climate zones, PV/grid/battery hybrid configurations consistently have lower NPCs than the grid-only option (Mohand Kaci et *al*., 2024). Similar results have also been observed in the agricultural sector, where a dairy farm in Tlemcen achieved an NPC of $106117.90 for its optimal hybrid system (Bouregba et *al.*, 2024).

3.10 Levelized Cost of Energy (LCOE)

The levelized cost of energy (LCOE) further confirms the economic competitiveness of the proposed system.The hybrid configuration achieves an LCOE of 4.40 DA/kWh, which is 22.3% lower than the grid electricity tariff, estimated at 5.66 DA/kWh. This indicates that, on average, each unit of electricity generated by the hybrid system costs less than electricity purchased from the public grid, which contributes significantly to the system's overall economic performance over the entire project lifespan.

These results are consistent with previous HOMER-based studies conducted in Algeria, where PV/grid/battery hybrid configurations consistently exhibit LCOEs lower than grid tariffs, with savings generally ranging between 15% and 35% depending on climatic zones and solar irradiation conditions (Mohand Kaci et *al.*, 2024). The reduction obtained in this study (22.3%) therefore falls within this range. Similar results have also been reported in the Algerian context, notably for a university system in Skikda with an LCOE of €0.193/kWh (Boucenna et *al.*, 2023).

Internationally, photovoltaic systems show a general downward trend in LCOE, confirming their growing competitiveness compared to conventional sources of electricity generation (Fraunhofer ISE, 2024).

3.11 Capital Expenditures (CAPEX)

The system's initial capital expenditures (CAPEX) amount to 16.7 million Algerian dinars, representing the initial investment required in year zero. This amount includes the cost of the 211 kW photovoltaic array, the 1612 batteries, the 54.1 kW converter, and the associated components of the rest of the system, including installation costs.

Although this represents a significant initial financial outlay, it must be viewed in the context of the system's long operational lifespan of 30 years. The CAPEX is effectively offset over time through reduced electricity purchases and operational savings, as reflected in the improved NPV and LCOE values mentioned earlier.

3.12 Cumulative Nominal Cash Flow

The cumulative nominal cash flow (Fig. 24) provides a temporal representation of the economic results mentioned earlier. It illustrates the evolution of total costs over the project's lifetime for the "grid-only" and "hybrid" configurations, confirming the long-term divergence in financial performance.

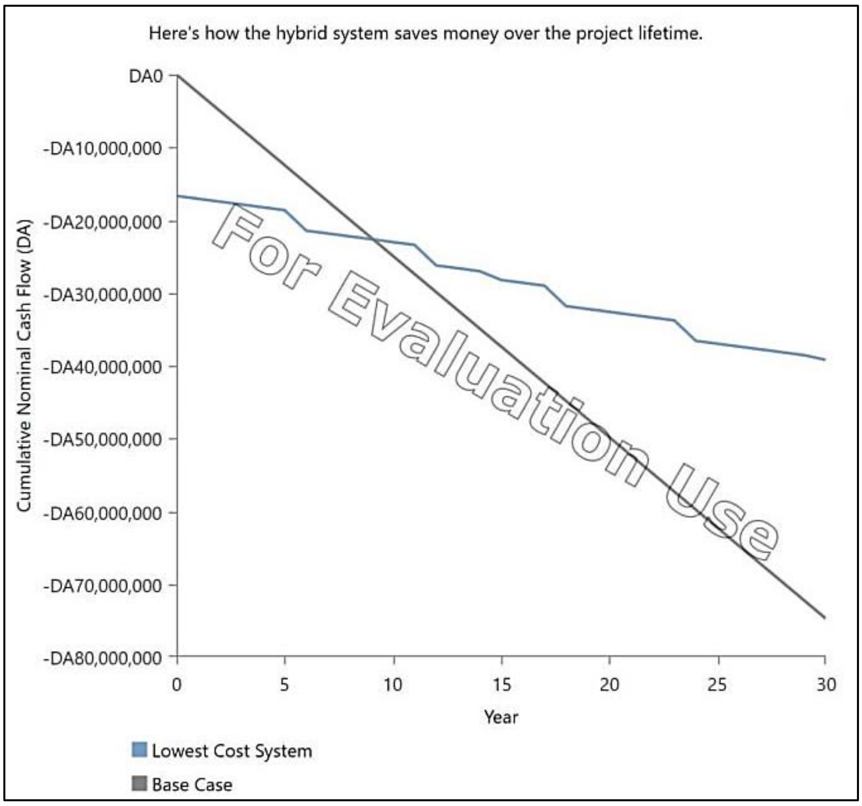

Figure 24. Cumulative nominal cash flow of the reference scenario and the lowest-cost system over 30 years

The hybrid system's initial negative position reflects the initial investment of 16.7 million DA, while the "grid-only" scenario starts at zero due to the absence of an initial investment. Over time, the hybrid system's curve rises at a slower rate, thanks to lower annual operating costs compared to the grid's ongoing electricity expenses.

As shown in Figure 26, the gap between the two systems gradually widens, reflecting the cumulative effect of reduced energy purchases and optimized operating costs. The periodic fluctuations in the hybrid curve are related to scheduled component replacements, particularly battery replacements, which result in one-time cost increases over the project's lifecycle.

The point where the curves intersect corresponds to the payback period, after which the hybrid system begins to generate a net economic benefit compared to the "grid-only" scenario. Beyond this point, the growing divergence between the two curves confirms the sustainable economic advantage of the hybrid configuration through the end of the project's lifespan.

The results presented in Table 4 indicate that the proposed hybrid system is economically viable based on the financial assumptions used. The internal rate of return (IRR) of 10% and the return on investment (ROI) of 7.1% confirm that the project generates positive financial returns throughout its lifespan, with the IRR exceeding the discount rate used in the analysis.

Table4 . Profitability indicators for the hybrid system

IRR	10%
ROI	7.1
Simple payback period (years)	9.1
Discounted payback period (years)	13.99
Present value of savings (DA/year)	7 685119
Annual value of savings (DA/year)	551 305

In terms of capital recovery, the system breaks even after 9.1 years according to the simple payback criterion, while the discounted payback period extends to 13.99 years when the time value of money is taken into account. Despite this increase, both values remain significantly lower than the project's 30-year lifespan, indicating a long operational period with a net financial benefit. The cumulative economic performance is further supported by a present value of savings of 7 685 119 DA and an annual value of 551 305 DA per year.

These results are consistent with previous technical-economic studies on grid-connected photovoltaic systems in Algeria, which indicate that projects are considered financially viable when IRR values exceed the discount rate and when acceptable payback periods and positive economic indicators are achieved (Mohand Kaci et *al*., 2024).

3.13 Cash Flow

The distribution of nominal cash flows that is, expenses and investments considered at their gross value as they occur is analyzed over a 30-year project lifespan. This analysis distinguishes the main components of the hybrid system: the photovoltaic array, the storage battery, the converter, and the electrical grid.

A peak in expenditures occurs in year 0 and corresponds to the initial investment in the photovoltaic array, the converter, and the storage system. Subsequently, recurring expenditures related to battery replacement occur approximately every six years. Another significant expenditure occurs around the fifteenth year, related to the replacement of the converter. At the same time, costs associated with the grid remain relatively stable over the entire study period. Finally, a positive net present value is observed in the thirtieth year; this corresponds to the last installed battery, which has not yet reached the end of its life (Fig. 25).

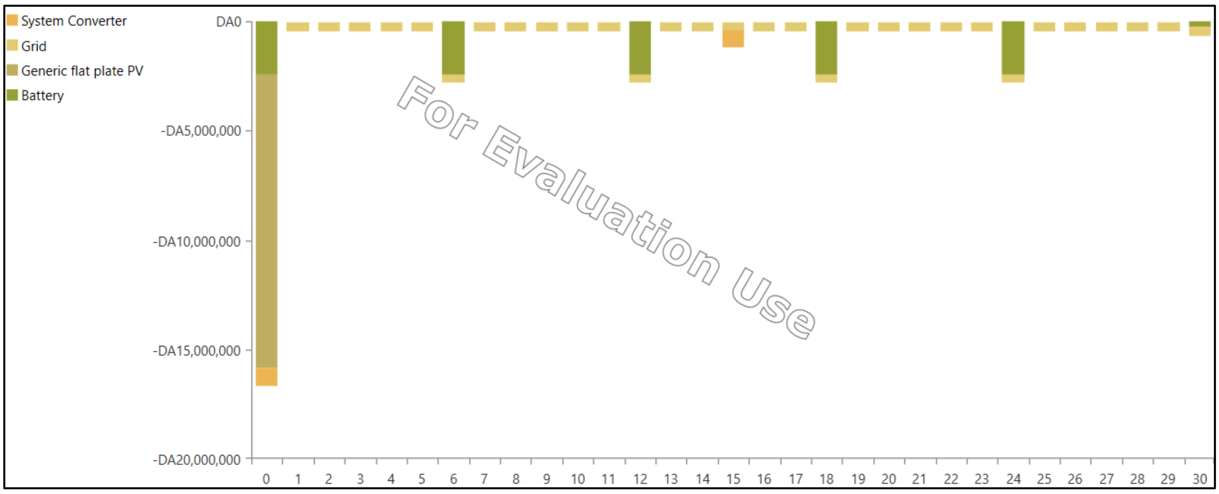

Figure 25. Nominal cash flows of the hybrid system over 30 years

3.14 Electricity Generation

Figure 26 illustrates the monthly energy contribution of the hybrid system's two power sources the photovoltaic panels and the utility grid expressed in kWh over a full year.

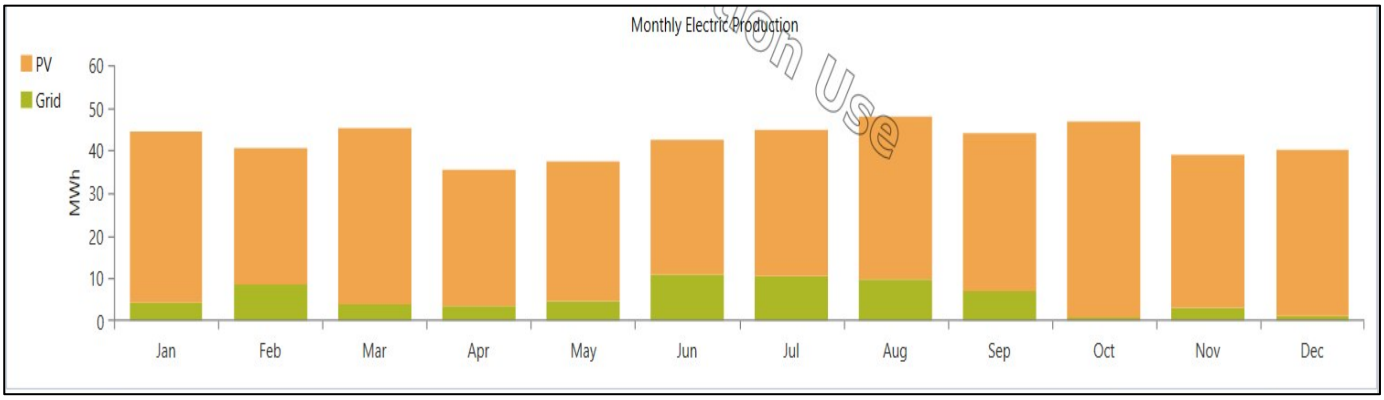

Figure 26. Monthly energy contribution of photovoltaic systems and the grid (kWh)

The monthly electricity generation profile shows a clear predominance of photovoltaic (PV) generation throughout the year, with the grid playing a secondary role in ensuring demand is met. PV generation remains the primary energy source every month, confirming a strong reliance on solar resources and efficient use of capacity.

3.15 Electric Power Flow

Table 5 presents the annual energy balance of the hybrid system, as estimated by HOMER Pro. It details the energy flows between the various generation sources and consumption destinations, allowing for an assessment of the system's overall efficiency and the degree to which demand is met.

Table5 . Electrical energy flows

Energy Source / Destination	kWh/year	Share (%)
Photovoltaic generation	439 366	86.6% of total supply
Purchases from the grid	68 047	13.4% of total supply
Total supply	507 413	100%
Primary load served	440 154	99.8% of consumption
Sales to the grid (export surplus)	728	0.165% of consumption
Electricity surplus (lost)	2 419	0.477% of generation
Unmet demand	0	0

The energy balance of the optimized hybrid system is summarized in the table above and reflects a strong predominance of photovoltaic (PV) generation throughout the year. The PV system produces 439 366 kWh/year, or 86.6% of the total energy supply, while grid purchases contribute 68 047 kWh/year (13.4%). This confirms that the system is primarily powered by solar energy, with the grid serving only as a backup source to ensure continuous operation.

The total electricity supplied amounts to 507 413 kWh/year, fully covering the primary AC load of 440 154 kWh/year, which corresponds to 99.8% of consumption, indicating near-total satisfaction of demand. A very small portion of the energy is either exported to the grid or lost due to system constraints. More specifically, 728 kWh/year (0.165%) are exported to the grid during periods of excess production, while 2419 kWh/year (0.477% of production) are classified as excess electricity (restriction).

Excess electricity occurs when photovoltaic production simultaneously exceeds both load demand and battery storage capacity, resulting in an inevitable reduction. However, this very low percentage (0.477%) reflects excellent system sizing with minimal waste. The 728 kWh/year exported to the grid represent a technically usable surplus, but under Algerian regulations (JORA, 2014), feed-in tariffs apply only to ground-mounted photovoltaic installations ≥ 1 MWp. Our system, at approximately 293 kWp, falls well below this threshold, and the negligible export revenues cannot justify the administrative burdens (20-year contract, annual report to the CREG, tariff renegotiation). In consequence, selling to the grid is not viable, and the system will operate in self-consumption mode (JORA, 2014).

More importantly, the system records no unmet load (0 kWh/year) over the entire simulation period (8760 hours), confirming total supply reliability. This result is essential for aquaculture applications, where an uninterrupted power supply is necessary for aeration, pumping, and water circulation systems, and where any power outage could have a direct impact on fish health and survival.

3.16 Share of Renewable Energy

To assess the effective contribution of renewable energy sources to the energy mix of the optimized hybrid system, HOMER Pro calculates two complementary indicators: the share of renewable energy, which measures the proportion of demand actually covered by photovoltaics, and the maximum penetration of renewable energy, which reflects the ratio of maximum instantaneous renewable production to load. The values obtained for the proposed system are presented in Table 6.

Table6 . Renewable energy share and maximum renewable energy penetration of the optimized system

Share of renewable energy	84.6%
Maximum penetration of renewable energy	506 %

The share of renewable energy is the most important sustainability indicator in this study, as it quantifies the proportion of total electricity demand supplied by renewable energy sources over the course of the year. In this case, 84.6% of the electricity consumed by the CNRDPA farm is supplied by the photovoltaic system, either directly during the day or indirectly via battery storage at night. The remaining 15.4% is supplied by the national grid.

A clear distinction must be made between the share of photovoltaic generation (86.6%) and the share of renewable energy (84.6%). The difference of approximately 2% is mainly attributed to energy losses within the storage system, particularly due to the round-trip efficiency of the batteries (approximately 80%). These losses occur during charge and discharge cycles, meaning that not all of the solar energy produced is actually supplied to the load. Consequently, the share of renewable energy provides a more realistic representation of usable renewable energy, rather than total production.

In this sense, the share of renewable energy reflects the proportion of the electrical load actually covered by renewable sources while accounting for all system inefficiencies. It is therefore a key performance indicator in hybrid energy systems, as it ensures an accurate assessment of renewable energy utilization beyond mere production figures (Bouregba et *al*., 2024).

3.17 Renewable Energy Penetration

3.17.1 Energy indicators

Energy indicators show a significant contribution from photovoltaic production (Table 7) to the overall operation of the hybrid system.

- Photovoltaic production covers 99.7% of the farm's energy demand.
- It accounts for 86.6% of the total energy generated by the system.

- Demand is fully met, with no energy deficit, as the “1 – non-renewable generation / load” indicator reaches 100%.

Table7 . Energy indicators of the PV-grid-battery hybrid system

Energy indicators	Value	Units
Total renewable production divided by load	99.7	%
Total renewable energy production divided by total production	86.6	%
Total non-renewable production minus total load	100	%

3.17.2 Instantaneous renewable production divided by the load

This graph shows the instantaneous proportion of photovoltaic production relative to the aquaculture farm’s energy demand, depending on the time of day and the day of the year (Fig. 27).

In summer, the absence of yellow areas between days 165 and 255 indicates that high demand absorbs almost all photovoltaic production, despite maximum irradiation levels.

In spring and fall, yellow zones appear around noon (approximately 12 p.m.), particularly between days 60 and 165 and then between 255 and 315. These reflect episodes of solar overproduction, which can exceed instantaneous demand several times over, with values exceeding 480% of the load.

In terms of coverage duration, the production period generally extends from 6–7 a.m. to 6–7 p.m. between days 60 and 315, with maximum duration in summer. In winter, this window is shorter and more concentrated around noon, reflecting lower solar radiation.

Overall, these results confirm strong seasonal variability: summer days are long and productive, but high demand limits the visibility of surplus production, while winter days are shorter and less productive.

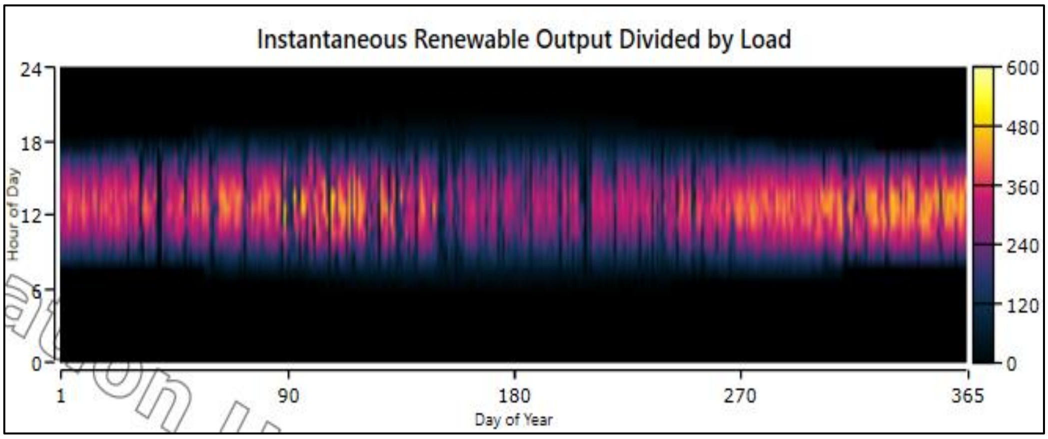

Figure 27. Instantaneous renewable production divided by load

3.17.3 Instantaneous Share of Photovoltaic Generation in Total Generation

This graph (Fig. 28) shows the instantaneous share of photovoltaic production in the hybrid system's total production, by time of day and day of the year.

During the night (from midnight to 6 a.m. and from 6 p.m. to midnight), the map appears uniformly black, indicating zero photovoltaic production and total reliance on the grid. During the day, primarily between 6–7 a.m. and 6 p.m., the predominance of yellow areas indicates that the energy produced comes mainly, if not entirely, from the photovoltaic array.

The duration of this peak contribution is shorter in winter, between days 1–60 and 315–365, when production extends approximately from 7–8 a.m. to 6 p.m. The rest of the year, this range extends from 6–7 a.m. until 7 p.m. or later, reflecting greater solar availability.

Purple areas also appear between days 165 and 270, especially in the early morning, when the photovoltaic share reaches about 60% of total production. Other intermediate shades, purple or orange, are observed more diffusely throughout the year and correspond to coverage levels between 60 and 80%.

Overall, these results highlight the high hourly and seasonal variability of photovoltaic production, while confirming the complementary nature of the solar array and the grid in the operation of the hybrid system.

The nighttime hours (12 a.m.–6 a.m. and 6 p.m.–12 a.m.) appear uniformly black, indicating zero photovoltaic production and total dependence on the power grid during these periods. In contrast, daytime hours (6 a.m.–7 a.m. and 6 p.m.) are predominantly colored yellow, corresponding to fully renewable production (100%), confirming that during daylight hours, all generated energy comes from the photovoltaic array.

The duration of this yellow shading, representing maximum solar production, is shorter between days 1–60 and 315–365 that is, in winter where production spans approximately (7–8 to 18) hours. The rest of the year, this duration lengthens and varies between 6–7 a.m. and 7 p.m. or later, reflecting increased energy availability during the summer.

We also observe areas of purple shading between days 165 and 270, corresponding to early morning, when the photovoltaic share reaches approximately 60% of total production. A few scattered bands of purple and orange hues appear throughout the year, indicating periods of intermediate cloud cover ranging from 60% to 80%.

These results highlight the high seasonal and hourly variability of photovoltaic production. Summer days are characterized by a long production duration and a high solar contribution, while winter periods have a shorter duration. The intermediate-colored areas reflect the transitions between production regimes, confirming the complementarity between photovoltaics and the grid in the operation of the hybrid system.

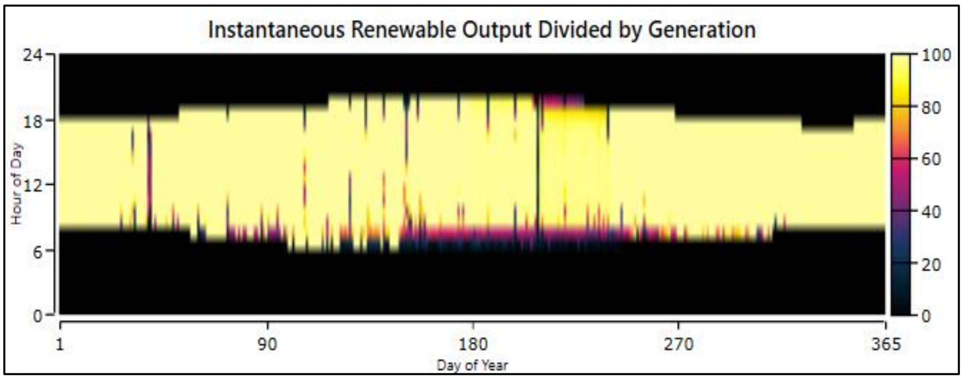

Figure 28. Instantaneous coverage of demand by photovoltaic production

3.18 Battery storage results

The heat map shows the daily charge-discharge pattern throughout the year (Fig. 29); daytime charging by the photovoltaic system appears as warm colors (yellow-red) concentrated between approximately 8 a.m. and 4 p.m., while nighttime discharge causes the battery to drop to its minimum state of charge (SoC) (blue-black).

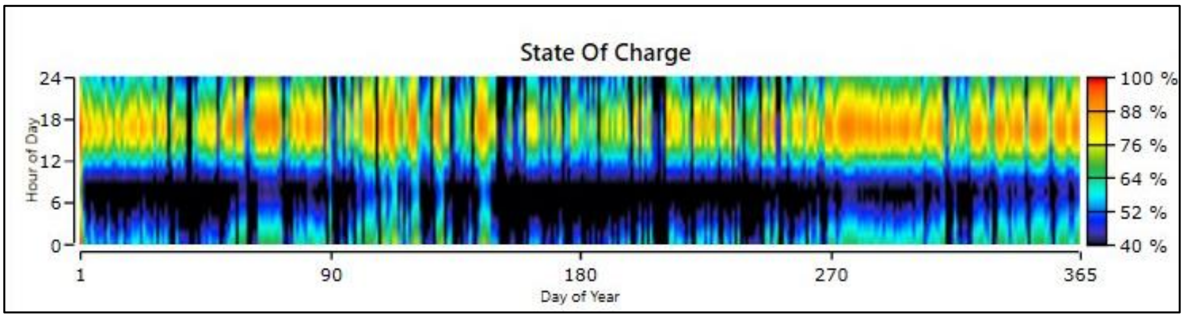

Figure 29. Battery state of charge by hour over the course of a year

This regular cyclic behavior is considered satisfactory for the system's operation (Lambert et *al.*, 2006). A seasonal variation is apparent: the summer months (days 150 to 270) show wider and more intense charging bands, corresponding to higher sunlight levels and longer days, while winter periods show weaker and delayed charging. The absence of persistent red zones (100% SoC) confirms minimal limitation of photovoltaic production, which is a favorable indicator of proper sizing of the photovoltaic system relative to storage (Notton et *al.*, 2018).

3.18.1 Battery Configuration

Table 8 presents the technical configuration of the battery bank selected by HOMER Pro following optimization. Compared to the initial input parameters of 112 batteries, the optimized system comprises 1612 batteries organized into 1612 single-unit parallel strings, with a bus voltage of 12 V, reflecting a significant increase in storage capacity to maximize renewable energy penetration.

Table8 . Technical specifications of the battery storage system

Quantity	Value	Unit
Batteries	1612	Quantity
Chain size	1.00	batteries
Parallel chains	1612	Chains
Bus voltage	12.0	V

3.18.2 Performance and Capacity Parameters

Table 9 summarizes the capacity and lifespan metrics of the optimized storage system, as estimated by HOMER Pro.

Table9 . Capacity, runtime, and lifespan characteristics of the battery system

Quantity	Value	Unit
Runtime	19.3	h
Storage wear cost	2.10	DA/kWh
Rated capacity	1613	kWh
Net rated capacity	968	kWh
Total output	1 289 600	kWh
Expected lifespan	5.87	years

The optimized battery bank has a nominal storage capacity of 1613 kWh, which corresponds to the total amount of energy that can theoretically be stored when the batteries are fully charged, going from a state of charge (SOC) of 0% to 100%. However, a minimum SOC limit of 40% has been imposed in HOMER, meaning that the batteries cannot discharge below 40% of their total capacity. This operational constraint is commonly applied to lead-acid batteries to prevent damage associated with deep discharge and to reduce degradation mechanisms such as irreversible sulfation, grid corrosion , and electrolyte stratification, which significantly shorten battery lifespan (Abreu *et al.*, 2016).

Consequently, only a portion of the nominal capacity is actually available to power the load.

Consequently, the effective usable capacity of the battery bank is reduced to 968 kWh, which corresponds to approximately 60% of the total nominal capacity. The application of a minimum SOC limit is considered a standard engineering practice in renewable energy storage systems to preserve battery integrity and extend their operational lifespan (Abreu *et al.*, 2016).

This storage capacity provides a runtime of approximately 19.3 hours, meaning that the battery bank alone can power the farm's load for nearly a full day in the absence of both photovoltaic generation and grid supply.

HOMER's battery lifespan model is based on a simplified version of the battery kinetic model, in which end-of-life is primarily determined by cumulative discharge in ampere-hours. Additionally, a service life parameter in float mode is imposed as an upper limit, regardless of operating conditions. This discharge-rate-based approach is generally considered conservative, as it does not fully account for external influencing factors such as operating temperature, charge/discharge rates, and maintenance conditions, which, in practice, can significantly affect battery degradation and result in actual lifetimes longer than those predicted by the model (Belfkira *et al.*, 2005).

In HOMER, the battery bank reaches the end of its service life when either the discharge limit specified by the manufacturer (800 kWh per battery × 1612 = 1 289 600 kWh) is exceeded, or the 6-year service life in float mode is reached, whichever comes first. In this case, the calculated lifespan of 5.87 years indicates that degradation is primarily driven by discharge rather than calendar aging, as the system operates at levels close to its design limits. This reflects a high-utilization storage configuration, in line with the objective of maximizing solar energy transfer and minimizing grid dependence.

Over the project's 30-year lifespan, this corresponds to approximately five planned replacement cycles. These replacements are already factored into the economic optimization via the annualized cost of 353 694 DA/year, which constitutes a significant component of the total system cost. Rather than representing a limitation, this cost reflects the essential role of the storage system in facilitating the high penetration of renewable energies and reducing dependence on grid electricity, thereby improving overall system performance and energy self-sufficiency.

Overall, the KBM framework provides a conservative estimate of battery lifespan and ensures rigorous planning of replacement cycles, while optimized operation confirms that the storage system is used effectively to support the long-term integration of renewable energy under reliable operating conditions (Belfkira *et al.*, 2005).

3.19 Flat-surface Photovoltaic Module

The installed photovoltaic system has a nominal capacity of 211 kW for a total annual production of 439366 kWh/year (Table 10). The average power is 50.2 kW, or approximately 1204 kWh/day, which corresponds to a load factor of 23.8% (Table 10). The simulation also indicates an observed maximum power of 231 kW, slightly higher than the nominal value, reflecting particularly favorable sunlight conditions. Finally, the system operates for approximately 4366 hours per year and achieves a photovoltaic penetration rate of 99.8%, demonstrating that the farm's energy demand is almost entirely covered by solar production (Table 11).

From an economic standpoint, the levelized cost of energy produced by the photovoltaic field is estimated at 2.21 DA/kWh (Table 11), confirming the system's competitiveness. No curtailed production was observed, meaning that all generated energy is utilized.

Table10 . Photovoltaic system production indicators

Quantity	**Value**
Rated power	211 kW
Average output	50.2 kW
Average output	1 204 kWh/day
Utilization rate	23.8%
Total production	439 366 kWh/year

Table11 . Performance and operational indicators

Quantity	**Value**
Minimum Output	0 kW
Maximum Output	231 kW
PV Penetration	99.8%
Hours of Operation	4 366 hrs/yr

Levelized cost	2.21 DA/kWh

Figure 30 illustrates the variation in photovoltaic power output based on the time of day and the day of the year. Power output ranges from 0 kW (dark areas) to approximately 231 kW (yellow areas), which corresponds to the maximum power observed.

The yellow areas, which correspond to periods of high production, are more concentrated between days 1–90 and 165–365. The duration of production is longer between days 60 and 315, extending approximately from 6–7 a.m. until 6–7 p.m., which corresponds to the time of year when sunny days are longest.

At the beginning and end of the day, power output is lower, represented by dark purple shades, corresponding to values between 50 and 100 kW. These zones reflect the gradual rise and decline in solar production.

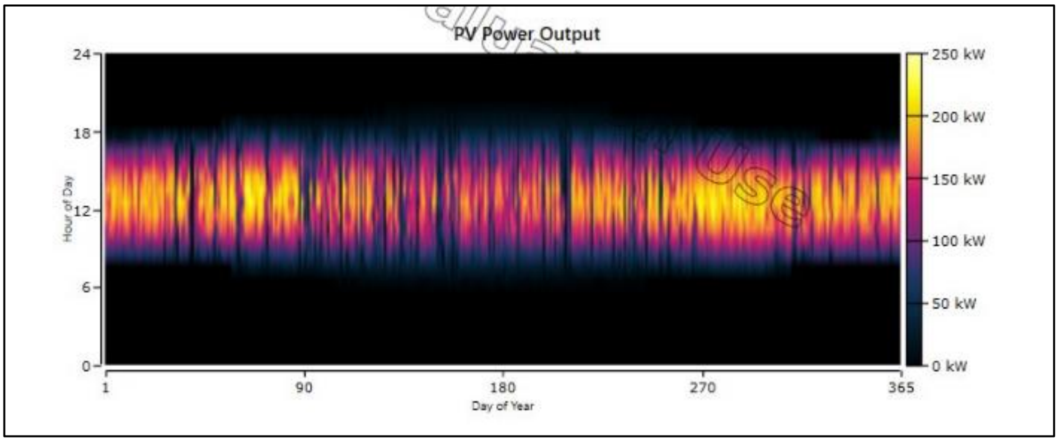

Figure 30. Hourly and seasonal variation in photovoltaic production

3.20 Grid

Table 12 summarizes the energy exchanges between the photovoltaic-battery system and the power grid.

Monthly loads vary by season, with peak values observed between June and August, a period marked by higher activity and increased consumption. Over the course of a year, energy purchased from the grid totals 68 047 kWh, while only 728 kWh is fed into the grid, corresponding to a photovoltaic surplus not stored by the battery.

These results show that the system is primarily geared toward self-consumption. Peak power remains generally stable, around 52 to 55 kW, while the annual bill amounts to 385 148 DA.

Table12 . Monthly energy exchanges with the grid

Month	Energy purchased (kWh)	Energy sold (kWh)	Net energy purchased (kWh)	Peak load (kW)	Energy cost (DA)	Demand charge (DA)
January	4200	19	4181	52	23 770.4	0
February	8654	7	8647	54	48 981.4	0
March	3732	50	3682	52	21 122.4	0
April	3483	127	3356	42	19 714.4	0
May	4541	130	4411	44	25 701.4	0
June	10927	0	10927	53	61 849.4	0
July	10622	0	10622	55	60 119.4	0
August	9883	52	9831	53	55 963.4	0
September	6935	4	6931	53	39 250.4	0
October	618	59	559	46	3496.2	0
November	3168	30	3138	48	17 751.4	0
December	1312	276	1037	40	7427.7	0
Annual	68047	728	67320	51	385 148	0

Figure 31 illustrates the amount of electricity imported from the grid based on the time of day and the day of the year. The color scale, ranging from 0 to 60 kW, reflects the intensity of the purchased power.

A distinct orange band appears between days 0 and 45, mainly between midnight and 7–8 a.m, reflecting increased reliance on the grid during winter. Another high-intensity zone is visible between days 160 and 270, during the summer, when energy demand rises due to thermal regulation needs and aquaculture activities.

Finally less intense orange bands are also observed between 6:00 p.m. and midnight, particularly around days 30 and 265. In contrast, the rest of the graph is dominated by black areas, indicating low or no energy imports.

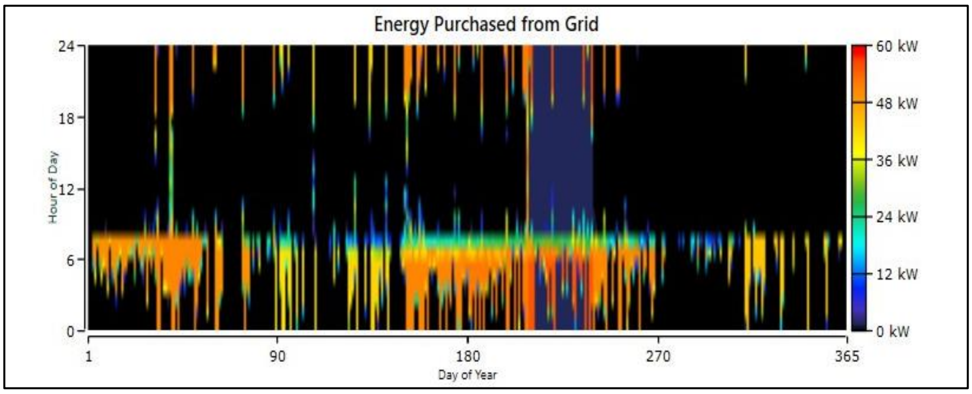

Figure 31. Daily and annual variation in energy purchased from the grid

3.21 Conversion System

The conversion system plays a central role in the operation of the hybrid system, ensuring the transformation of energy between DC and AC components. HOMER Pro sizes and evaluates the converter in terms of capacity, utilization rate, and annual energy balance. The capacity indicators for inverters and rectifiers are presented in Table 13, while the operational and energy indicators are detailed in Table 14.

Table13 . Capacity indicators for inverters and rectifiers s of the hybrid system

Quantity	Inverter	Rectifier
Capacity	54.1 kW	54.1 kW
Average power	42.6 kW	0 kW
Minimum power	0 kW	0 kW
Maximum power	54.1 kW	0 kW
Utilization rate	78.6%	0%

Table14 . Operational and energy indicators of the hybrid system

Quantity	Inverter	Rectifier
Operating hours	8415 h/year	0 h/year
Energy generated	372834 kWh/year	0 kWh/year
Energy consumed	388369 kWh/year	0 kWh/year
Losses	15535 kWh/year	0 kWh/year

3.21.1 Inverter Performance

This graph (Fig. 32) illustrates the inverter's operation throughout the year and by hour of the day, highlighting variations in power output by time period:

- Orange bands appear mainly between days 1–90 and 165–290, indicating high power output, exceeding 48 kW and approaching the converter's maximum capacity.
- This consistent demand shows that the system relies heavily on DC-to-AC conversion to utilize photovoltaic generation and directly supply the load.
- The yellow bands observed during the rest of the year correspond to intermediate power levels, generally ranging from 36 to 48 kW.
- Darker areas appear between 12 a.m. and 7 a.m. throughout the year, as well as more sporadically between 6 p.m. and midnight, indicating periods of lower output.

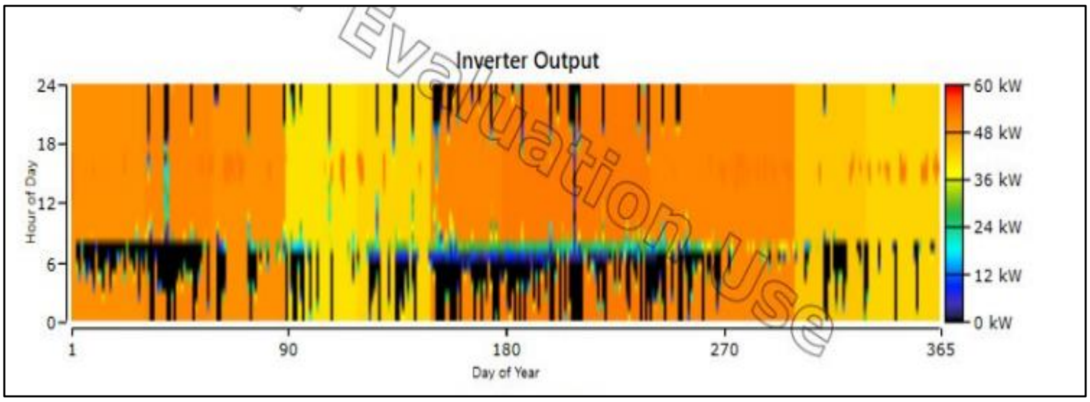

Figure 32. Hourly and seasonal distribution of inverter output power (kW**)**

3.21.2 Rectifier Behavior

The map (Fig. 33) appears entirely black, confirming the absence of rectifier activity throughout the simulation period.

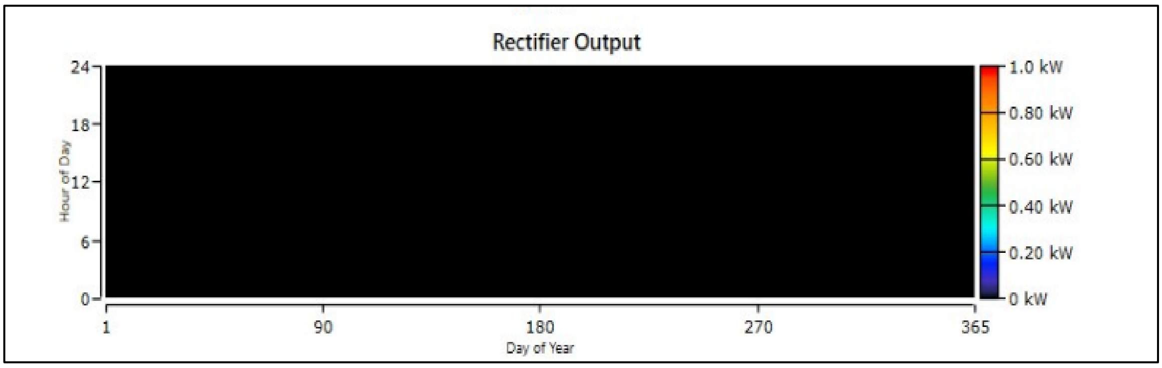

Figure 33. Hourly and seasonal distribution of rectifier output power (kW)

3.22 Emissions

Table 15 presents the annual atmospheric emissions associated with each system configuration, as calculated by HOMER Pro based on the emission factors for grid electricity and the annual energy purchased from the public grid. The “grid-only” reference scenario draws all 440154 kWh/year from the grid, while the PV/battery hybrid system requires only approximately 155454 kWh/year of grid purchases, representing a reduction of about 64.7% in grid consumption thanks to the high share of renewable energy provided by the 211 kW PV array.

Emissions are calculated by HOMER by multiplying the annual grid energy consumption by the emission factors specific to the pollutants associated with the local grid’s generation mix (Lambert et *al.*, 2006).

Table15 . Annual atmospheric emissions (reference scenario and hybrid system)

Pollutant	Grid alone (kg/year)	Hybrid system (kg/year)	Reduction (kg/year)	Reduction (%)
Carbon dioxide (CO_2)	278177	42546	−235631	84.7
Sulfur dioxide (SO_2)	1206	184	−1022	84.7
Nitrogen oxides (NO_x)	590	90.2	−499.8	84.7

3.22.1 Carbon Dioxide Emissions

The most significant environmental benefit of the hybrid system (Table 15) is the 84.7% reduction in annual CO_2 emissions, which drop from 278177 kg/year (grid alone) to 42546 kg/year (hybrid system). This reduction is directly proportional to the decrease in grid electricity consumption and is consistent with the grid CO_2 emission factor incorporated into the HOMER Pro simulation (Lambert et *al.*, 2006). The 235631 kg/year of CO_2 avoided is a figure of considerable environmental and regulatory significance in the context of Algeria’s Nationally Determined Contribution (NDC) under the United Nations Framework Convention on Climate Change (UNFCCC), in which Algeria has committed to achieving a 27% share of renewable energy in its national electricity mix by 2030, subject to international support (Climate Watch, n.d.). The CO_2 emissions avoided documented here contribute directly to the achievement of these mitigation goals.

3.22.2 Sulfur Dioxide and Nitrogen Oxide Emissions

SO_2 and NO_x emissions are reduced by 84.7%, in direct proportion to the reduction in grid electricity consumption, falling from 1206 kg/year and 590 kg/year (grid alone) to 184 kg/year and 90.2 kg/year (hybrid system), respectively. SO_2 comes from the combustion of sulfur-containing fossil fuels in the combustion chambers of thermal power plants, while NO_x results from the oxidation of nitrogen at high temperatures during combustion (Seinfeld & Pandis, 2016).

Although the absolute quantities are modest compared to point source industrial emissions, their local and regional health implications should not be overlooked. SO_2 is a recognized precursor of fine particulate matter ($PM_{2,5}$) through atmospheric oxidation into sulfate aerosols, which are associated with cardiovascular and respiratory morbidity (Seinfeld & Pandis, 2016; WHO, 2021). NO_x contributes to the formation of tropospheric ozone and has been independently associated with the burden of respiratory disease in urban and peri-urban populations (WHO, 2021). The World Health Organization's updated global air quality guidelines set annual average concentration limit values of 5 µg/m³ for $PM_{2,5}$ and 10 µg/m³ for NO_2, reflecting the severity of health impacts even at low pollutant concentrations (WHO, 2021).

The zero values recorded for carbon monoxide, unburned hydrocarbons, and particulate matter in both system configurations reflect the inherently clean combustion profile of natural gas-fired electricity generation, unlike coal- or heavy fuel oil-fired grids where these pollutants constitute a significant portion of the total atmospheric load (IEA, 2021). This characteristic of the Algerian grid limits the scope of the hybrid system's associated pollution benefits to CO_2, SO_2, and NO_x only.

3.23 A Photovoltaic-Based Irradiance Monitoring and Operator Alert System

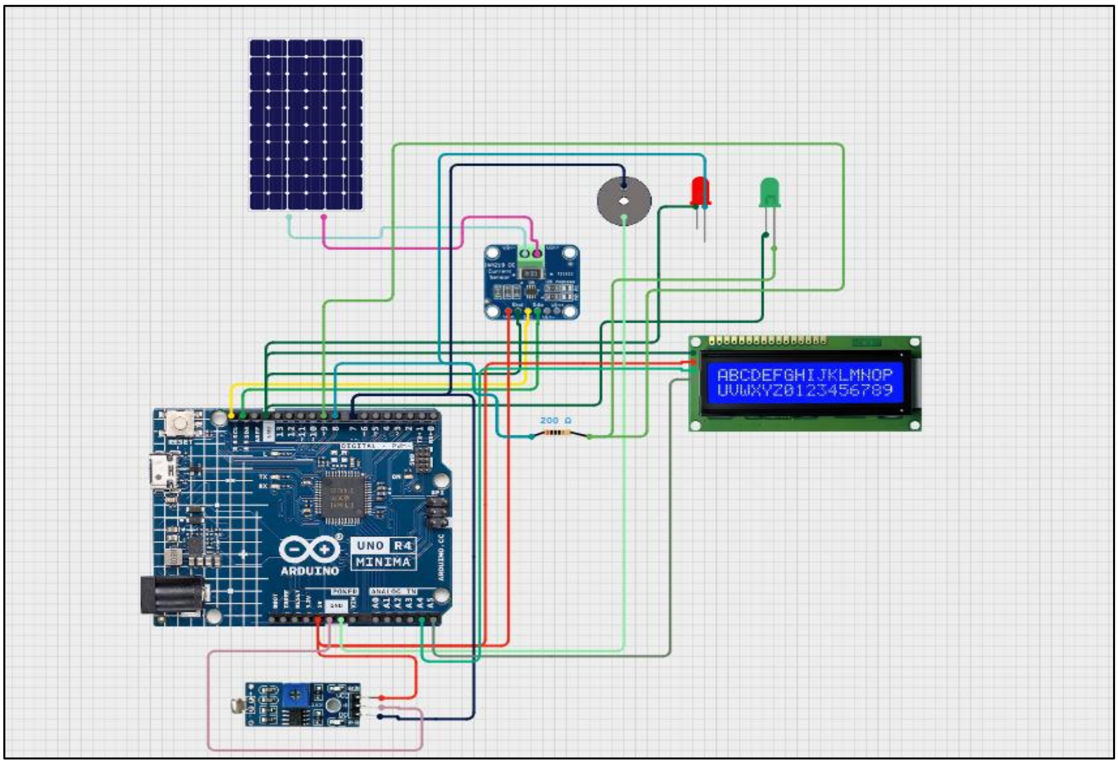

Figure 34. Proposed circuit schematic of the solar irradiance monitoring and alert system designed using Cirkit Designer IDE

The proposed monitoring and alert system (Fig. 34) represent a low-cost, operator-oriented decision-support tool designed to bridge the gap between solar energy availability and aquaculture farm operations. The circuit design integrates real-time power measurement via the INA219 sensor with a three-level alert logic: at high irradiance, the system activates the green LED, triggers an audible double-beep alert, and displays the message "RUN BACKWASH NOW" on the LCD screen; at medium irradiance, normal operational conditions are indicated; at low irradiance, the red LED warns operators to reduce non-essential energy consumption. The system requires no cloud connectivity or complex infrastructure, making it suitable for deployment in Algerian aquaculture farms with limited technical resources. Physical prototyping and field validation are identified as a direct continuation of this work.

Conclusion

Conclusion

The CNRDPA experimental farm, although small in size and partially operational, exhibits significant energy consumption when active, exacerbated by frequent outages and environmental impacts linked to the exclusive use of the electrical grid. To address this issue, a hybrid system combining photovoltaics, the grid, and batteries was proposed and sized. The energy modeling, optimized and simulated using HOMER Pro, was supplemented by an economic and environmental assessment.

The study showed that, given the region's high solar potential and the continuous energy needs of aquaculture systems, a hybrid solution is both practical and advantageous.

The optimal system includes a 211 kW photovoltaic array, 1.6 MWh of storage capacity, and a 54.1 kW converter. Compared to the "grid-only" scenario, it reduces the overall life-cycle cost by 22.1%, lowers the cost of electricity by 22.3%, and reduces annual operating costs by more than 70%.

From an environmental perspective, the system significantly reduces CO_2 emissions by approximately 85%, as well as SO_2 and NO_x emissions, thereby contributing to Algeria's climate and energy goals. Despite these solid results, the study has certain limitations, notably the assumption of a uniform hourly load profile that does not reflect actual consumption variations, as well as the use of data limited to a single reference year and a reduced lifespan of lead-acid batteries. Future improvements could include the use of lithium batteries, the integration of another renewable energy source suitable for the site, better demand management, and the use of more accurate real-world data. A more in-depth economic and environmental analysis, including sensitivity studies and a comprehensive life-cycle assessment, is also recommended.

Perspectives

Additional economic and environmental analyses, including sensitivity studies and comprehensive life-cycle assessments, are recommended to strengthen the evaluation of the proposed system. Overall, this study demonstrates that hybrid renewable energy systems represent a viable, cost-effective, and sustainable solution for aquaculture facilities and could be replicated in similar facilities in Algeria, thereby contributing to the development of a low-carbon blue economy.

Although conducted on an experimental farm, this approach can be applied to commercial aquaculture farms or larger processing facilities, where energy consumption is much higher. A hybrid photovoltaic–grid–battery system would allow them to reduce their dependence on the grid and significantly lower their energy costs.

This model is also particularly well-suited to sites isolated from the power grid, such as remote rural or coastal areas, where full solar coverage is often the only reliable solution to ensure continuous production. Integrating renewable energy into such facilities would help reduce operational costs, strengthen energy security, and improve the environmental sustainability of intensive aquaculture.

Given Algeria's exceptional solar potential in the Saharan interior, extending the hybrid solar-powered RAS model developed in this study to off-grid desert sites represents a promising research perspective, this would position solar-powered intensive aquaculture as a viable contributor to food security in Algeria's arid interior regions.

Bibliographic References

Bibliographic References

1. Abreu, P. H., Pires, V. F., & Foito, D. (2016). Operating conditions of lead-acid batteries in the optimization of hybrid energy systems and micro-grids. *Solar Energy, 139*, 697–713. https://doi.org/10.1016/j.solener.2016.10.007
2. Ayer, N. W., & Tyedmers, P. H. (2009). Assessing alternative aquaculture technologies: Life cycle assessment of salmonid culture systems in Canada. *Journal of Cleaner Production, 17*(3), 362–373. https://doi.org/10.1016/j.jclepro.2008.08.002
3. Badiola, M., Basurko, O. C., Piedrahita, R. H., Hundley, P., Mendiola, D., & Bostock, J. (2018). Energy use in recirculating aquaculture systems (RAS): A review. *Aquacultural Engineering, 81*, 57–70. https://doi.org/10.1016/j.aquaeng.2018.03.003
4. Baz, N., & Laouas, F. (2025). Study of the energy efficiency of aquaculture farms (Master's thesis, Houari Boumediene University of Science and Technology).
5. Belfkira, R., Hajji, B., & Tironi, E. (2005). Lead-acid battery lifetime modeling in hybrid renewable energy systems. https://www.researchgate.net/publication/246687286
6. Bendaas, I., Bouchouicha, K., Bouchakour, S., Boulahchiche, S., Razagui, A., Semaoui, S., & Hadj Arab, A. (2025). Performance degradation and economic resilience of grid-connected PV systems in desert climates. *Renewable Energy*. https://www.sciencedirect.com/science/article/abs/pii/S0960148125027089
7. Bharathi, S., Antony, C., Uma, A., Ahilan, B., Aanand, S., & Sunder Lingam, R. S. (2019). Application of renewable energy in aquaculture. *Aquaculture International Magazine*.
8. Biswas, D., Ali, M. F., Saha, M., Alam, M. S., Ali, M., AlAqil, M. A., Obaidi, O., & Islam, M. K. (2026). Techno-economic optimization of hybrid microgrids. *Scientific Reports, 16*, 7695.
9. Bouguerra, F. (2023). *Overview of aquaculture in Algeria*. Ministry of Agriculture.
10. Boucenna, K., Sebbagh, T., & Benchouia, N.-E. (2023). Hybrid PV-wind-fuel cell system optimization. *JESA, 56*(1), 1–12. https://doi.org/10.18280/jesa.560104
11. Bouregba, H., Hachemi, M., Samatar, A. M., et al. (2024). Feasibility of PV/wind hybrid system. *Heliyon, 10*(23), e40650.
12. Cai, J., Galli, G., & Zhou, X. (2023). Aquaculture growth potential in Algeria. FAO.
13. Climate and Clean Air Coalition. (2025). *The health burden of fossil fuels*. https://climateandhealthalliance.org/wp-content/uploads/2025/09/C2G-FR_EXE-SUMMARY.pdf

14. Climate Watch. (n.d.). Algeria NDC. https://www.climatewatchdata.org/ndcs/country/DZA/full
15. CNRDPA. (2026). National Center for Fisheries and Aquaculture Research and Development. https://www.CNRDPA.dz/cnrpda/
16. David, P., Pop, A., & Popovici, V. (2009). Energy efficiency in recirculating aquatic systems. *AACL Bioflux*.
17. Dodo, U. A., et al. (2024). Battery energy storage in hybrid systems. *Energy, 304*, 132140. https://doi.org/10.1016/j.energy.2024.132140
18. Emezirinwune, M. U., Achebe, C. H., & Okolie, S. T. A. (2024). Smart aquaponics system. *Sustainable Energy Technologies and Assessments*. https://doi.org/10.1016/j.seta.2025.033
19. FAO. (2022). RAS parameters and aquaculture systems.
20. Fezzani, A., Guermoui, M., Kouzou, A., et al. (2023). Grid-tied PV plants in Algeria. *Sustainability, 15*(19), 14282. https://doi.org/10.3390/su151914282
21. Food and Agriculture Organization of the United Nations. (2024). *The state of world fisheries and aquaculture 2024*. https://doi.org/10.4060/cd0683en
22. Fraunhofer Institute for Solar Energy Systems ISE. (2024). *Photovoltaics Report*. https://www.ise.fraunhofer.de/...
23. Funge-Smith, S., & Phillips, M. J. (2001). Aquaculture systems typology.
24. Guidi, G., Violante, A. C., & De Iuliis, S. (2023). Environmental impact of electricity generation. *Energies*.
25. Haddad, S., & Boulahchiche, S. (2025). Solar PV development in Algeria. *AJESS*.
26. Hakima Kaddour. (2024). Solar energy production in Algeria. CDER.
27. Hana Saada. (2024). FAO praises Algeria's progress in aquaculture. https://www.dzair-tube.dz/en/fao-commends-algerias-aquaculture-progress/
28. Hasnaoui, A., & Benrouissi, A. (2018). Solar cell simulation using COMSOL.
29. HOMER Energy. (2020). *HOMER Pro brochure*. https://homerenergy.com/static/pdf/Homer-Pro-Brochure.pdf
30. International Energy Agency (IEA). (2021). *Algeria – Key energy statistics*. https://www.iea.org/countries/algeria
31. IEA. (2025). *Global Energy Review 2025*.
32. IEA. (2025). *World Energy Outlook 2025*. https://www.iea.org/reports/world-energy-outlook-2025

33. IPCC. (2023). *Climate Change 2023: Synthesis Report*. https://doi.org/10.59327/IPCC/AR6-9789291691647
34. Isaac, E. A. (2025). Renewable energy in aquaculture operations. *African Journal*. https://doi.org/10.70382/ajbegr.v8i4.022
35. Jangampalli Adi Pradeepkiran. (2019). Aquaculture and food security. *Translational Animal Science*.
36. Lalwani, M., Kothari, D. P., & Singh, M. (2010). PV simulation software review.
37. Lambert, T., Gilman, P., & Lilienthal, P. (2006). HOMER modeling. Wiley-IEEE Press.
38. Macknick, J., Newmark, R., Heath, G., & Hallett, K. C. (2012). Water use in electricity generation. *Environmental Research Letters*.
39. Mekuye, B., et al. (2024). Energy systems overview.
40. Marion, B., Adelstein, J., & Boyle, K., et al. (2005). PV system performance parameters. NREL.
41. Mohand Kaci, G., Mahrane, A., Ghedamsi, K., & Chikh, M. (2024). PV feasibility in Algeria. *Energy & Environment*. https://doi.org/10.1177/0958305X221146953
42. Notton, G., Lazarov, V., & Stoyanov, L. (2018). PV system sizing optimization. *Renewable Energy, 116*, 1041–1051. https://doi.org/10.1016/j.renene.2017.09.087
43. Odeh, S. (2018). PV performance indicators. *Journal of Power and Energy Engineering*.
44. Official Journal of the Algerian Republic, dated April 23, 2014.
45. Osman, A. I., et al. (2022). Renewable energy impacts. *Environmental Chemistry Letters*.
46. OECD & FAO. (2025). *Agricultural outlook 2025–2034*. https://doi.org/10.1787/601276cd-en
47. Raji, L., Razak, A. A., & Sharol, A. F. (2025). Comparison of PV simulation tools. *Next Energy*.
48. Royal Society of Chemistry. (2025). Electricity access.
49. Scroggins, R. E., et al. (2022). Renewable energy in fisheries. *Journal of Cleaner Production*.
50. Seinfeld, J. H., & Pandis, S. N. (2016). *Atmospheric chemistry and physics*. Wiley.
51. Tokyo Institute of Technology. (2025). Electricity access.
52. UNECE. (2022). Natural gas emissions.

53. University of Maryland Extension. (2023). Solar system design guide. https://extension.umd.edu/resource/working-solar-design-and-system-sizing-fs-2023-0655
54. United Nations. (2022). Renewable energy transition. https://www.un.org/en/climatechange/raising-ambition/renewable-energy-transition
55. U.S. Department of Energy (DOE). (2024). *Crystalline Silicon Photovoltaics Research*. https://www.energy.gov/eere/solar/crystalline-silicon-photovoltaics-research
56. WHO. (2021). WHO Air Quality Guidelines. https://www.who.int/publications/i/item/9789240034228
57. Vo, T. T. E., Ko, H., Huh, J.-H., & Park, N. (2021). Solar energy for aquaculture. *Energies, 14*(21), 6923. https://doi.org/10.3390/en14216923